이학박사학위논문

Decoherence Effects on All-optical Quantum Information Processing

전 광학적 양자정보처리에 대한 결깨어짐 효과

2012년 8월

서울대학교 대학원

물리천문학부

박 기 민

Decoherence Effects on All-optical Quantum Information Processing

전 광학적 양자정보처리에 대한 결깨어짐 효과

지도교수 정 현 석

이 논문을 이학박사 학위논문으로 제출함

2012년 08월

서울대학교 대학원

물리천문학부

박 기 민

박기민의 이학박사 학위논문을 인준함

2012년 08월

위 원 장 안 경 원 (인)

부위원장 정 현 석 (인)

위 원 김 형 도 (인)

위 원 신 용 일 (인)

위 원 이 진 형 (인)

Decoherence Effects on All-optical Quantum Information Processing

Kimin Park

Supervised by

Associate Professor **Hyunseok Jeong**

A Dissertation

Submitted to the Faculty of

Seoul National University

in Partial Fulfillment of

the Requirements for the Degree of

Doctor of Philosophy

August 2012

Department of Physics and Astronomy

Graduate School

Seoul National University

Abstract

It has been thought for long that information is something useful but does not have physical reality, irrelevant to physical laws. Landauer's principle concerning the entropy increase accompanying the erasure of a bit implies that this belief is not true. The recent developments in quantum information processing (QIP) have brought the advantages inaccessible for classical means, such as unconditionally secure communication, exponential speed-ups in factoring integers and database search.

Optical QIP, using light for information carrier, has been a popular choice among many candidates due to the significant developments in photon manipulation. In addition, it is easy to combine communication and computation using light. Linear optics using only passive optical elements (e.g. beam splitter) which conserve energy of the states is of interest, as naturally occurring non-linearity is very small.

Decoherence caused by the openness of the system of interest is nowadays considered as a major factor of the occurrence of classicality out of quantum physics. Decoherence destroys coherence inevitable for quantum aspect of information, and is a big obstacle for QIP.

In this thesis, the focus will be put on the effect of decoherence on the optical QIP, particularly on the quantum teleportation proposed by Bennett *et al.*, which is one of the core ingredient of linear optical QIP. Quantum teleportation can be a very efficient way to implement quantum gate operations, and thus the degradation on it will affect the efficiency of total quantum circuit.

I will introduce the two works related to this topic. First, we study entangled coherent states versus entangled photon pairs for practical quantum-information processing. We compare effects of decoherence and detection inefficiency on entangled coherent states (ECSs) and entangled photon pairs (EPPs), both of which are known to be particularly useful for quantum information processing. When decoherence effects caused by photon losses are heavy, the ECSs outperform the EPPs as quantum channels for teleportation both in fidelities and in success probabilities. On the other hand, when inefficient detectors are used, the teleportation scheme using the ECSs suffers undetected errors that result in the degradation of fidelity, while this is not the case for the teleportation scheme using the EPPs. Our study reveals the merits and demerits of the two types of entangled states in realizing practical QIP under realistic conditions.

Secondly, we study quantum teleportation between two different types of optical qubits, one of which is "particle-like" and the other "field-like," via hybrid entangled states under the effects of decoherence. We find that teleportation from particle-like to field-like qubits can be achieved with a higher fidelity than that in the opposite direction. However, teleportation from field-like to particle-like qubits is found to be more efficient in terms of the success probabilities. Our study shows that the direction of teleportation should be considered an impor-

tant factor in developing optical hybrid architectures for quantum information processing.

Keywords: Quantum Information Processing, Quantum Teleportation, Decoherence, Optical Quantum Communication

Student Number: 2006-30768

Contents

List of Figures

Chapter 1

Introduction

A thought that information is something useful but does not necessarily have physical reality, nor is governed by physical laws was the idea hidden behind a well-known paradox called Maxwell's demon [1]. In this paradox, a demon is able to separate a hot molecules from cold ones into two different rooms without no other resources than the information about the molecules, thus violating the second law of thermodynamics. Landauer's principle [2] concerning the entropy increase accompanying the erasure of a bit, however, implies that this belief is not true. The physical law should govern the dynamics of information, which enables the superposition, entanglement and nonlocality of information governed by quantum physics. This idea was what inspired Feynman, who proposed to use "quantum information" in computational or simulational tasks [3]. The recent developments in quantum information processing (QIP) have brought the advantages inaccessible by classical means, such as unconditionally secure communication[4], exponential speed-ups in factoring integers and database search [5, 6].

Two basic theorems of QIP are stated in the form of so-called the *no-cloning*

theorem [7] and *no-signalling* theorem [8]. The two theorems are related in a sense that the violence of one theorem would inevitably lead to the violation of the other, and both of them contribute to guarantee the nonlocality of the quantum mechanics not leading to the violation of the special relativity. To mention the theorems briefly, the no-cloning theorem states that there exists no such operation that allows $|\psi\rangle|0\rangle \rightarrow |\psi\rangle|\psi\rangle$ for an arbitrary state $|\psi\rangle$, and the no-signalling theorem states that no physical effect can be instantaneously induced on a physical system by another system isolated from it. The two theorems are related as follows: if cloning is possible, together with a quantum teleportation [160], one person can send a signal at a speed faster than a light. On the other hand, if a signalling scheme exists, it can be repeated in a clever way to reconstruct a quantum state. More recently, nevertheless, an imperfect cloning was proven to be possible [10].

Optical QIP, using light for information carrier, has been an active area of research among many candidates [11] due to the significant developments in photon manipulation. In addition, it offers a platform easy to combine communication and computation using light [12]. Linear optics using only passive optical elements (e.g. beam splitter) which conserve energy of the states is of recent interest, as naturally occurring non-linearity is very small [13].

Decoherence is nowadays spotted as one of major factors of the occurrence of classicality out of quantum physics [14]. It is caused by the openness of the system of interest, arising from the information transfer by the interaction between system and the environment. Decoherence destroys coherence inevitable for quantum aspect of information, and is a big obstacle for QIP [15]. Quantum error

correction codes [16] are one of the main methods to prevent the decoherence.

In this thesis, the focus will be put on the effect of decoherence on the optical QIP, particularly on the quantum teleportation [160], which is one of the core ingredient of linear optics [12]. It was first proposed by Bennett *et al.*, as a quantum method of sending information without any corresponding classical analogues. It was pointed out in [17] that teleportation can be a very efficient tool for a method to implement quantum gate operations, and thus the degradation on it will affect the efficiency of the entire quantum circuit.

I will introduce the two works related to this topic. First, entangled coherent states versus entangled photon pairs for practical quantum-information processing [169]. Second, quantum teleportation between dual-rail and single-rail qubits. We will compare the efficiency of teleportations in two optical QIP schemes in a realistic situation, and will evaluate the effectiveness of a strategy of using teleportation to combine those two schemes in the same situation.

The structure of this thesis is as follows. In Chapter 2, a brief description of the quantum entanglement is presented. In Chapter 3, decoherence theory is described, which is adopted to model the environmental effect. Two schemes of optical QIP, using photons and coherent states as information carriers, are explained in Chapter 4. The main works of this thesis are summarized in Chapter 5 and 6. We conclude in Chapter 7 with final remarks and prospect.

Chapter 2

Entanglement

After the birth of quantum mechanics, it was recognized that the quantum entanglement [19] which enables a strange "spooky action at a distance [20]," was not a special occurrence in quantum mechanics, but occupies a larger space than the set of separable states, which may not seem to be in accordance with our everyday experiences as well as Einstein's theory of relativity which allows only the local interactions, and has been a topic of intense debate by physicists ever since [21]. Nowadays such a quantum correlation, i.e. quantum entanglement, is generally accepted in theoretical sense, and also being harnessed as a central resource in quantum information processing.

2.1 Applications with entanglement

For a pure state residing in n subsystem Hilbert space, the total state of the system is called entangled if it is written in terms of the basis states $|i_j\rangle$ in

subsystem j as

$$|\psi\rangle = \sum_{i_1,...i_n} c_{i_1,i_2,...,i_n} |i_1\rangle \otimes |i_2\rangle \otimes ... |i_n\rangle \neq |\psi_1\rangle \otimes ... |\psi_n\rangle \,, \tag{2.1}$$

but not in the product form [19]. Thus each subsystem does not possess a single state vector in this case. A mixed state is entangled if it cannot be written as a convex combination of product states [22]

$$\rho \neq \sum_i p_i \rho_1^i \otimes ... \otimes \rho_n^i, \tag{2.2}$$

although a new quantum correlation weaker than entanglement, quantum discord, has been discovered recently [23].

Entanglement between subsystems makes some tasks feasible which are not accessible by any classical means. As the first example, clever use of Bell's inequality [24] can be used to share a private cryptographic key in unconditionally secure ways [25]. The protocol is based on the insight that the measurement performed by the eavesdropper Eve will introduce elements of physical reality to the measurements, thus the Bell inequality cannot be violated.

Another paradoxical phenomenon by the utilization of entanglement is the entanglement between the particles which have never interacted in the past, by the procedure called entanglement swapping [26]. It is performed as follows. Alice and Bob share a maximally entangled state $|\phi^+\rangle_{AB_1} = 1/\sqrt{2}(|0\rangle_A |0\rangle_{B_1} + |1\rangle_A |1\rangle_{B_1})$, while Bob also shares another maximally entangled state $|\phi^+\rangle_{B_2C}$ with Charlie

such that the total state is

$$\left|\phi^{+}\right\rangle_{AB_1} \otimes \left|\phi^{+}\right\rangle_{B_2C}, \tag{2.3}$$

and thus, after Bob performs a joint measurement in the Bell basis and tell the outcome to Alice and Charlie, they are able to perform local unitary rotations to obtain the entangled state $|\phi^{+}\rangle_{AC}$.

The last example but not the least of importance is quantum teleportation [160]. It is a quantum way to communicate an unknown qubit without violating well-known theorems in quantum computation. Suppose Alice and Bob share a maximally entangled state and they can communicate classically. The shared entangled state is, for example, given as

$$|B_1\rangle_{AB} = \frac{1}{\sqrt{2}}\big(\,|0\rangle_A\,|0\rangle_B + |1\rangle_A\,|1\rangle_B\,\big), \tag{2.4}$$

and Alice wants to send a qubit $|\psi\rangle_{A'} = a\,|0\rangle_{A'} + b\,|1\rangle_{A'}$. The total state $|\Psi\rangle = |\psi\rangle_{A'} \otimes |B_1\rangle_{AB}$ can also be written in Bell basis of mode $A - A'$, i.e. $|B_i\rangle = (U_i)_A\,|B_1\rangle_{A'A}$ where $U_i = \{I, \sigma_z, \sigma_x, \sigma_x\sigma_z\}$ with Pauli matrices:

$$\begin{aligned}|\Psi\rangle =& \frac{1}{2}\Big(\,|B_1\rangle_{A'A}\,(a\,|0\rangle_B + b\,|1\rangle_B) + |B_2\rangle_{A'A}\,(a\,|0\rangle_B - b\,|1\rangle_B)\\ &+ |B_3\rangle_{A'A}\,(b\,|0\rangle_B + a\,|1\rangle_B) + |B_4\rangle_{A'A}\,(b\,|0\rangle_B - a\,|1\rangle_B)\Big),\end{aligned} \tag{2.5}$$

where each state of mode B in the parenthesis corresponds to the Bob's conditional state when Alice obtains the Bell measurement outcome as the corresponding state in $A' - A$. Alice tells Bob about her results. After applying unitary rotations (indepedent of a and b as a and b are unknown arbitrary values), Bob

obtain the qubit $|\psi\rangle_B = a|0\rangle_B + b|1\rangle_B$ in mode B identical to the Alice's original in mode A', the explicit form of the unitary operations is identity operator I, Pauli operators σ_z, σ_x and σ_y in the orders of $|B_1\rangle_{A'A}$, $|B_2\rangle_{A'A}$, $|B_3\rangle_{A'A}$ and $|B_4\rangle_{A'A}$. Quantum teleportation is different from the direct transmission of the particle, in that the modes Alice and Bob hold are different, thus the physical form may be completely transformed by the teleportation, even though the information contained in the output mode is the same with the input mode, and also that Alice only has to use classical communication at the time she wants to send the quantum information. These properties are advantageous in quantum information processing, which will be discussed later.

2.2 Nonlocal character of entanglement

The fact that entanglement is different from classical correlation implies the existence of the tests that cannot be explained by the latter, which are usually referred to as Bell's inequality tests [27]. One famous example is the so-called CHSH inequality [28], which involves two dichotomic measurements and a bipartite correlation experiment. It is written as

$$B_{av} = |E(a,b) - E(a,b') + E(a',b) + E(a'b')| \leq 2, \tag{2.6}$$

where a and a' (b and b') are detector settings on A (B) side, and $E(a,b)$ is the correlation (average value of the joint measurement) of settings a and b. This inequality specifies the bound for the value of any local hidden variable model (LHV) [29], while quantum mechanics predicts a different bound violating the

above inequality, namely Cirel'son inequality [30] $B_{av} \leq 2\sqrt{2}$, where B_{av} is now obtained according to quantum mechanics. It was proved later that CHSH inequality violation condition is equivalent to entanglement condition for projective measurements in bipartite systems [31].

In contrast to the statistical nature of the above inequality, there exists a test of quantum formalism that can be performed with a single measurement for which LHV predicts completely differently. This type of nonlocality test, or "Bell theorem without inequalities" are manifested in [32] using the tri-partite entangled GHZ state $1/\sqrt{2}(|000\rangle + |111\rangle)$. Experiments related to this type of nonlocality test have been performed using two-photon hyperentanglement [33] and linear cluster state [34].

The *holistic* nature of entangled state is revealed also by entropic description where the von Neumann entropy $S = -\mathrm{Tr}(\rho \log \rho)$ of a subsystem can be greater than the von Neumann entropy of the total system [35], which can be written in bitartite system as

$$S(\rho_A) + S(\rho_B) \geq S(\rho_{AB}), \tag{2.7}$$

where $\rho_{A,B,AB}$ represents the reduced density matrix of subsystem A, B and the total density operator, where the equality holds for product states. It also has been proven that for systems without entanglement, the following inequality holds [36, 37] which can also be interpreted as a separability criteria:

$$S_\alpha(\rho_{AB}) \geq S_\alpha(\rho_A), \quad S_\alpha(\rho_{AB}) \geq S_\alpha(\rho_B), \tag{2.8}$$

where $S_\alpha = (1-\alpha)^{-1} \log \mathrm{Tr}\rho^\alpha$ is the α Renyi entropy, a generalized version of

van Neumann entropy.

Operational meaning of quantum conditional entropy

$$S(A|B) = S(\rho_{AB}) - S(\rho_B) \tag{2.9}$$

has been provided recently in terms of state merging [38], which is related to the amount of quantum communication necessary to construct the total state for Bob who initially had part of the state. What is paradoxical is that the conditional entropy may have negative values, which is also a signature of entanglement. The interpretation is that the result of the state merging produce, instead of consume, pairs of maximally entangled state equal to $-S(A|B)$.

There has been efforts to tell whether a given state is entangled or not. In terms of bipartite pure states, all states that cannot be written as a product form are entangled, which is equivalent to having a single nonzero Schmidt coefficient. For mixed bipartite states, the separability condition is identical to the possibility to be written as the following form as was denoted above:

$$\rho_{AB} = \sum_{i=1}^{k} p_i \rho_A^i \otimes \rho_B^i, \tag{2.10}$$

where ρ_A^i's and ρ_B^i's are local density operators. It is known that the set of all such separable states is convex, compact and invariant under arbitrary local unitary operations such as $U_A \otimes U_B$.

A necessary condition for separability, is often called Peres's positive partial transpose criterion [39]. It is summarized as follows: for all separable states, after

partial transposition (PT)

$$\rho_{AB} = \sum_{i=1}^{k} p_i \rho_A^i \otimes \rho_B^i \xrightarrow{PT} \sigma_{AB} = \sum_{i=1}^{k} p_i (\rho_A^i)^T \otimes \rho_B^i, \tag{2.11}$$

where σ is a valid density matrix, which means that all of its eigenvalues are positive. What is notable about this criteria is that it is stronger than all entropic criteria based on Renyi α entropy, and is a necessary-sufficient condition for separability of the $2 \otimes 2$ and $2 \otimes 3$ cases.

2.3 Quantification of entanglement

Quantifying the amount of entanglement is important in QIP, because we have to know how much resource we have with a certain given state in order to perform a task properly. Thus it is related to the question how useful the state is, and we give a brief summary of the measures of entanglement.

Entanglement distillation [40] is a protocol that changes a n copies of state ρ into the target states (usually the maximally entangled state) $|\phi^+\rangle^{\otimes m_n}$ by means of local operations and classical communications (LOCC) λ. Distillable entanglement is the supremum of the rate of distillation $r = \lim_n m_n/n$, which can be written formally:

$$E_D(\rho) = \sup\{r : \lim_{n\to\infty} [\inf_{\Lambda} ||\Lambda(\rho^{\otimes n}) - (|\phi_+\rangle \langle\phi_+|)^{\otimes rn}||] = 0\}, \tag{2.12}$$

where $||\cdot||$ is the trace norm. There also exists a measure dual to $E_D(\rho)$ called entanglement cost (cf. [41]).

There exist axiomatic approaches obtained from functions satisfying some postulates, different from the above measures obtained from optimization of certain protocols. Monotonicity of entanglement which states that entanglement cannot increase under LOCC, first proposed by [42], is written as

$$\forall \Lambda \in \text{LOCC}, \quad E(\Lambda(\rho)) \leq E(\rho). \tag{2.13}$$

This postulate was claimed to be the only postulate necessary for entanglement measures [43]. Other postulates are often imposed on the measures, nowadays being thought as optional. Important ones are that entanglement must vanish on separable states, or that it is equal to e-bits for maximally entangled states, namely $E((\Phi^+)^{\otimes n}) = n$, or that it is continuous on Hilbert space such that $||\rho - \sigma|| = 0 \Rightarrow |E(\rho) - E(\sigma)| = 0$ for two arbitrary states ρ and σ which is called asymptotic continuity, or that it is convex.

Negativity and concurrence are two popular entanglement measures, which will be discussed briefly here. Concurrence [44, 45] for bipartite two qubit state ρ is give as

$$C(\rho) = \max\{0, \lambda_1 - \lambda_2 - \lambda_3 - \lambda_4\} \tag{2.14}$$

where λ_i's are eigenvalues of matrix $R = \sqrt{\sqrt{\rho}(\sigma_y \otimes \sigma_y)\rho^*(\sigma_y \otimes \sigma_y)\sqrt{\rho}}$ with σ_y is a Pauli matrix. A good property of concurrence is that it satisfies the so-called monogamy inequality [46]:

$$C(\rho_{AB})^2 + C(\rho_{AC})^2 \leq C(\rho_{A(BC)})^2, \tag{2.15}$$

where ρ_{AB} and ρ_{AC} are reduced density matrices of the tripartite state ρ_{ABC} and

$C(\rho_{A(BC)})$ is the concurrence between mode A and joint mode BC. Concurrence is also related to entanglement of formation [45].

Another popular measure, negativity [167, 168] is related to PPT criteria mentioned above. It is written as:

$$N(\rho) = \sum_{\lambda<0} |\lambda|, \tag{2.16}$$

where λ is the eigenvalues of partial transposed density matrix ρ^{PT}. This measure has many advantages: it is LOCC monotone, and is related to the upper bound of distillable entanglement and the teleportation capacity, thus gauge the amount of useful entanglement for QIP purposes [168]. As will be noted later, this measure will be the main quantity of entanglement measure in this thesis.

2.4 Quantum steering

Another facet of nonlocality has drawn attention recently, the concept of quantum steerability [49] inspired by Schrödinger's famous paper in 1935 [50]. Quantum steerability can be concisely stated as the ability to control a remote particle separated in a relativistic sense so that there exists no classical means to affect it. The scenario where quantum steerability is revealed is depicted as follows [51]. Alice sends a particle to Bob who doubts that quantum mechanics can work nonlocally in the way that Alice can control the particle she sent. Bob now picks out one of the two complementary observables in a random manner, e.g. position or momentum, and challenge Alice to predict the outcome of the measurement Bob will perform. If Alice predicts better than the bound allowed by any local theo-

ries, Bob has to admit that Alice has manifested her nonlocal controllability over Bob's particle, i.e. quantum steerability. The bound is what was recently given by Wiseman *et al.* [49], and the equivalence of EPR paradox and quantum steering was shown in [52]. A recent experimental evidence of loop-hole free quantum steerability was reported in [51].

Chapter 3

Decoherence

Classical mechanics under the assumptions of locality limited by relativistic theories and reality which allows the existence of *objective* physical properties independent of an observer, has been pointed out to have a discrepancy with quantum mechanics with a nonlocal character revealed by Bell inequality [27] and *non-realistic* properties fundamentally imposed by Heisenberg uncertainty principle [53]. It is necessary that, therefore, a reconciliation between them must take place in some ways to avoid the incompatibility, or at least the inconsistency, in order to describe the world with unified laws of physics.

3.1 Conceptual importance

It is often claimed that quantum mechanics is more fundamental than classical mechanics (for example, refer to [54]), and the latter can be exhibited by considering only the former, but there has not existed an agreed answer about the mechanism how a quantum object turns into classical. Among many candi-

dates for this problem [55, 56, 57], decoherence process has been often adopted as an ingredient in these approaches, but nowadays it has become an independent description of how the classicality is born out of the quantumness [58, 14]. In this section, decoherence theory will be treated as an interpretation of quantum mechanics to give answers to the important problems.

3.1.1 Decoherence

In brief, the decoherence process [14, 58] can be summarized as a process by which a pure quantum state becomes a classical mixture by the ubiquitous interaction with the environment (cf. [59, 60]). Two important aspects of decoherence according to [14] which are also related with each other can be stated as environmental-induced decoherence (fast local suppression of interference) and environment-induced superselection (selection of preferred sets of states). They will be discussed below in more detail in relation to the paradoxes in quantum theory.

3.1.2 Measurements, the preferred basis problem and environment-induced superselection

According to Copenhagen interpretation of quantum mechanics, when a quantum state $|\psi\rangle = a\,|0\rangle + b\,|1\rangle$ is measured about some basis $\{|0\rangle, |1\rangle\}$, the result is only one of the two states, not both, with probabilities given from Born rule as $|a|^2$ and $|b|^2$. However, three hidden (unanswered) questions exist: i) what chooses the basis of the measurement, and how? ii) why is the result state given as only one of the two, and not the superposition? iii) exactly what picks out one of the

two? In specific, i) is called the preferred basis problem, and the definite outcome problem is concerned with ii).

Before proceeding to how the decoherence theory explains about these problems, let's describe the von Neumann scheme to enlighten the problems in more detail. A system of interest S in a superposition state $\sum_n c_n |s_n\rangle$ interacts with the measuring apparatus A in the state $|a_0\rangle$ to become an entangled state between S and A in the form of $\sum_n c_n |s_n\rangle |a_n\rangle$. The preferred basis problem is revealed by the fact that generally there does not exist a unique representation of the $S-A$ entangled state when c_n's are uniform. For example, the following state can be written in many ways (two prominent bases were written explicitly):

$$\frac{1}{\sqrt{2}}\big(|0\rangle |0\rangle + |1\rangle |1\rangle \big) = \frac{1}{\sqrt{2}}\big(|+\rangle |+\rangle + |-\rangle |-\rangle \big), \tag{3.1}$$

where $|\pm\rangle = 2^{-1/2}(|0\rangle \pm |1\rangle)$, thus it is ambiguous about which basis this apparatus is actually measuring. It is also evident that which outcome was chosen is not presented at all in this representation. The preferred basis problem in decoherence program is explained by the addition of a environment beside the system and the apparatus. The $S-A$ entangled state interacting with the environment in $|e_0\rangle$ suffers the following process:

$$(\sum_n c_n |s_n\rangle |a_n\rangle) |e_0\rangle \longrightarrow \sum_n c_n |s_n\rangle |a_n\rangle |e_n\rangle , \tag{3.2}$$

where the uniqueness of the final form is guaranteed [61], also known as tridecompositional uniqueness theorem. Additional criteria also exists, which is called the stability criterion [60]. It means that the system-apparatus correlation $|s_n\rangle |a_n\rangle$

should be stable against the apparatus-environment interaction Hamiltonian $\hat{H}_{\mathrm{AE}}$, which can be also written as

$$\forall n,\ [\hat{P}_n = |s_n\rangle \langle s_n|, \hat{H}_{\mathrm{AE}}] = 0. \tag{3.3}$$

We can say that the above condition describes a situation where the preferred-basis (or pointer basis) is determined by the environment.

3.1.3 Environmental-induced decoherence

Decoherence, i.e. local suppression of interference [14], is another aspect of the environment-induced superselection. When the system in the state $\sum_n c_n |s_n\rangle$ interacts with the environment in state $|e_0\rangle$, a system-environment entanglement is generated to make $\sum_n c_n |s_n\rangle |e_n\rangle$, where $|e_n\rangle$ are not necessarily mutually orthogonal. The reduced density matrix of the system by taking partial trace of the environmental mode is given as:

$$\rho_S = \sum_{n,m} c_n c_m^* |s_n\rangle \langle s_m| \otimes \langle e_m|e_n\rangle. \tag{3.4}$$

When $\langle e_m|e_n\rangle \to \delta_{n,m}$ asymptotically, the state becomes $\rho_S = \sum_n |c_n|^2 |s_n\rangle \langle s_n|$. When compared with the initial state $\sum_n c_n |s_n\rangle$, you notice that a quantum superposition has turned into a classical mixture. It is also notable that there exists no physical difference between the two above-mentioned aspects of decoherence, as both describes the entanglement with the environment and the consequences of it.

3.2 Mathematical description of decoherence

3.2.1 Born and Markov Approximations

The decoherence process can be derived from the Schrödinger equation for the total state of the system and the environment. However, due to the inaccessibility of the state of the environment, many assumptions are made on the state and the properties of environment, and the equation for the reduced density matrix of the system is used instead as in [62]. The evolution of the reduced density matrix of the system at time t in initial state $\rho_S(0)$ under environment is written as

$$\rho_S(t) = \mathrm{Tr}_E[\hat{U}(t)\rho_{SE}\hat{U}^\dagger(t)] = \hat{V}(t)\rho_S(0), \tag{3.5}$$

where $\hat{U}(t)$ is the time-evolution for the composite system, and $\hat{V}(t)$ is a dynamical map of above written in superoperator form. The differential equation of the above evolution local in time, i.e. when the equation has no other time dependence than t, is written as:

$$\frac{\mathrm{d}}{\mathrm{d}t}\rho_S(t) = \hat{L}\rho_S(t), \tag{3.6}$$

where superoperator $\hat{L}$ usually depends on initial state of the environment and at time t.

Two approximations are usually made for the decoherence processes, so-called Born-Markov approximations. They are adopted for a simple environment without *weirdness*, and are described as ([63]):

The Born approximation The system-environment coupling is sufficiently weak

and the environment is large enough. The consequence of this approximation is that the system and the quasi-stable environment is in an approximate product state at all times $\rho(t) \approx \rho_S(t) \otimes \rho_E$.

The Markov approximation The environment is *memory-less*, so that self-correlations of the environment decay sufficiently fast. This assumption is the origin of the time locality.

3.2.2 Master equation of optical dissipative process

Here I will give a brief derivation of so-called Lindblad form of the master equation describing a dissipative process under Born-Markov approximations following [62].

The density matrix of the system interacting with the environment can be written in the form of quantum Liouville equation

$$\frac{\mathrm{d}}{\mathrm{d}t}\rho_{SE}(t) = -\frac{i}{\hbar}[\hat{V}_I(t), \rho_{SE}(t)], \tag{3.7}$$

where $\hat{V}_I(t) = i\hbar\big(\hat{s}^\dagger \hat{F}(t) - \hat{F}^\dagger(t)\hat{s}\big)$ is the interaction Hamiltonian with system operator $\hat{s}$ and the environmental Langevin operator $\hat{F}(t)$. We look at only the system by taking partial trace in the environmental degree of freedom as before, i.e. $\rho_S(t) = \mathrm{Tr}_E(\rho_{SE}(t))$. Substituting the formal integration of (3.7) from 0 to t

into itself using explicit form of $\hat{V}_I(t)$ gives:

$$\begin{aligned}\frac{\mathrm{d}}{\mathrm{d}t}\rho_S(t) &= -\frac{i}{\hbar}\mathrm{Tr}_E[\hat{V}_I(t), \rho_{SE}(0)] - \frac{1}{\hbar^2}\int_0^t \mathrm{d}t' \ \mathrm{Tr}_E[\hat{V}_I(t), [\hat{V}_I(t'), \rho_{SE}(t')]] \\ &= \int_0^t \mathrm{d}t' \ \mathrm{Tr}_E[\hat{s}^\dagger \hat{F}(t) - \hat{F}^\dagger(t)\hat{s}, [\hat{s}^\dagger \hat{F}(t') - \hat{F}^\dagger(t')\hat{s}, \rho_E(0) \otimes \rho_S(t')]], \quad (3.8)\end{aligned}$$

where we used the Born approximation explicitly to the form of $\rho_{SE}(t) = \rho_E(0) \otimes \rho_S(t')$. In the derivation of the second line (3.8) the assumption of environment in thermodynamic equilibrium was used so that excitation $\mathrm{Tr}_E\big(\rho_E(0)\hat{F}(t)\big) = 0$ deletes the first term of the first line, $\mathrm{Tr}_E[\hat{V}_I(t), \rho_{SE}(0)] = 0$. It can be simplified further by considering that all averages containing unequal numbers of creation operators $\hat{F}$ and annihilation operators $\hat{F}^\dagger$ vanishes under the environment in thermodynamic equilibrium, and using (5.5.24) and (5.5.25) in [62], you obtain

$$\begin{aligned}\frac{\mathrm{d}}{\mathrm{d}t}\rho_S(t) = \int_0^t \mathrm{d}t' \int \mathrm{d}\Delta \ W^2(\Delta)\Big\{ &[\hat{s}\rho_S(t')\hat{s}^\dagger - \hat{s}^\dagger\hat{s}\rho_S(t')][\bar{n}(\Delta)+1]\exp[-i\Delta(t-t')] \\ &+ [\hat{s}\rho_S(t')\hat{s}^\dagger - \rho_S(t')\hat{s}^\dagger\hat{s}][\bar{n}(\Delta)+1]\exp[i\Delta(t-t')] \\ &+ [\hat{s}^\dagger\rho_S(t')\hat{s} - \hat{s}^\dagger\hat{s}\rho_S(t')]\bar{n}(\Delta)\exp[i\Delta(t-t')] \\ &+ [\hat{s}^\dagger\rho_S(t')\hat{s} - \rho_S(t')\hat{s}^\dagger\hat{s}]\bar{n}(\Delta)\exp[-i\Delta(t-t')]\Big\}, \quad (3.9)\end{aligned}$$

where $W(\Delta)$ is the coupling at frequency Δ and $\bar{n}(\Delta)$ is the mean occupation number. Markovian approximation enters at this stage, the overall effect of which is such that the Δ integral is sharply peaked at t, changing the t' integral into a simple expression where all t''s are replaced with t, and the Δ integral is guaranteed to have convergence, having the form of the principal value integrals.

Eq. (3.9) now changes into

$$\begin{aligned}\frac{\mathrm{d}}{\mathrm{d}t}\rho_S(t) &= -i\delta\omega[\hat{s}^\dagger\hat{s},\rho_S(t)] - i\delta\omega_{\mathrm{th}}\big[[\hat{s}^\dagger,\hat{s}],\rho_S(t)\big] \\ &+ \Gamma[\bar{n}(0)+1][2\hat{s}\rho_S(t)\hat{s}^\dagger - \hat{s}^\dagger\hat{s}\rho_S(t) - \rho_S(t)\hat{s}^\dagger\hat{s}] \\ &+ \Gamma\bar{n}(0)[2\hat{s}^\dagger\rho_S(t)\hat{s} - \hat{s}\hat{s}^\dagger\rho_S(t) - \rho_S(t)\hat{s}\hat{s}^\dagger], \end{aligned} \tag{3.10}$$

where $\Gamma = \pi W^2(0)$, $\delta\omega = -\mathbb{P}\int \mathrm{d}\Delta\, W^2(\Delta)/\Delta$ and $\delta\omega_{\mathrm{th}} = -\mathbb{P}\int \mathrm{d}\Delta\, \bar{n}(\Delta)W^2(\Delta)/\Delta$. The first two terms are usually small compared to the other terms, and if not, they only cause the frequency shifts of natural frequency of the system. The final form of the master equation is

$$\begin{aligned}\frac{\mathrm{d}}{\mathrm{d}t}\rho_S(t) &= \Gamma[\bar{n}(0)+1][2\hat{s}\rho_S(t)\hat{s}^\dagger - \hat{s}^\dagger\hat{s}\rho_S(t) - \rho_S(t)\hat{s}^\dagger\hat{s}] \\ &+ \Gamma\bar{n}(0)[2\hat{s}^\dagger\rho_S(t)\hat{s} - \hat{s}\hat{s}^\dagger\rho_S(t) - \rho_S(t)\hat{s}\hat{s}^\dagger]. \end{aligned} \tag{3.11}$$

For optical systems, the environment is usually thought of as zero temperature and the system operator is given as the annihilation operator $\hat{a}$, and the master equation is reduced to

$$\frac{\mathrm{d}}{\mathrm{d}t}\rho_S(t) = \Gamma[2\hat{a}\rho_S(t)\hat{a}^\dagger - \hat{a}^\dagger\hat{a}\rho_S(t) - \rho_S(t)\hat{a}^\dagger\hat{a}] \equiv 2\Gamma(\hat{J}+\hat{L})\rho_S(t), \tag{3.12}$$

where $\hat{J}\rho = \hat{a}\rho\hat{a}^\dagger$ and $\hat{L} = -(\hat{a}^\dagger\hat{a}\rho + \rho\hat{a}^\dagger\hat{a})/2$.

3.2.3 Non-markovian dynamics

There exist situations where Born-Markov approximations does not hold, i.e., either the system-environment coupling is strong or memory effect exists in the

environment. For example, a superconducting qubit strongly coupled to a low-temperature environment made of spin baths does not satisfy Born-Markov approximations [64]. Integro-differential equations are required to describe such systems, and the so-called Nakazima-Zwanzig projection-operator approach [65, 66] is often adopted.

3.3 Decay rate of optical decoherence

Optical states such as photons or lasers, which are mathematically described by Fock states or coherent states in an ideal sense, are assumed to be either flying freely or confined in a closed structure such as optical cavities. In real world experiments, however, they usually suffer imperfections, or interact with the environment, so they do not retain their initial forms. Decays may occur to diminish the amplitudes, or decoherence may occur to decrease their purity.

In optical cavity, the mirrors which consist of the cavity walls are not perfectly reflecting, and there exist photons that are leaked probabilistically. In optical fiber or in air, there exist atoms or impurities that scatter off the travelling lights. These processes occur at different rates depending on the mechanisms. For example, the attenuation in air occurs mainly due to the Rayleigh scattering, and the exponential decay rate is $\gamma_a \approx 1.8 \times 10^2 s^{-1}$ (calculated from the data in [67]). In optical fiber, the decay rate is $\gamma_f \approx 1.2 \times 10^4 s^{-1}$ [68]. The decay rate of the optical cavity is comparatively fast, a typical figure of $2.69 \times 10^8 s^{-1}$ [69]. The decays of the coherent amplitudes in these systems are shown in Fig. (3.1).

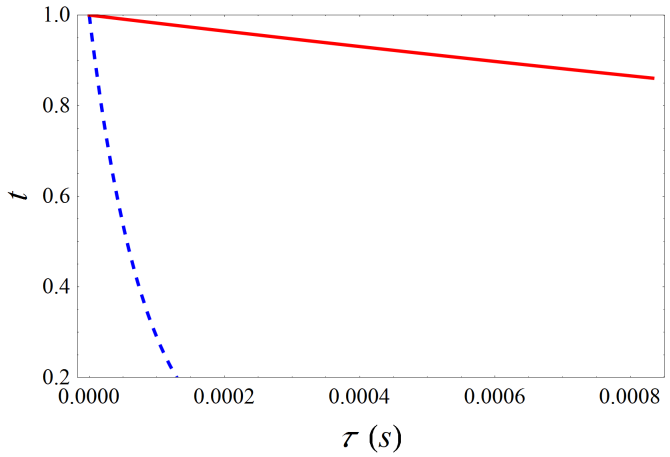

Figure 3.1: Exponential decay of the coherent amplitude against time. The Rayleigh scattering in air is drawn in solid red line, and the decay in optical fiber is drawn in dashed blue line.

Chapter 4

Optical Quantum Information Processing

If a quantum state can be in a superposition state, is the information contained in the state also superposed? If so, would a faster computation be possible using such an "superposition of information"? This is related to the concept of quantum computer first proposed by Feynman [3], and has been answered in confirmative ways since then. Computation with photons [12, 70], which Feynman has taken as the first example, is the topic of this chapter.

4.1 Linear optical quantum computation

There exist many candidates for the hardwares of quantum information processing, the prominent examples of which are ion-trap, superconducting qubits, nuclear magnetic resonance, quantum dots, photons and etc. (for a review, refer to [71]), and each of them has different advantages and shortcomings. Quantized particles of optical systems (photons) are relatively easy to be conveyed with less

effect of decoherence due to the lack of photon-photon interaction Hamiltonian, which may be an advantage in communications as well as an difficulty of the implementation of two-qubit quantum gates. KLM protocol [144] adopted teleportation of two-photon gates [17] to achieve scalable quantum computing with linear optics and projective measurements. Recently one-way quantum computation using cluster states [73] have been developed besides the quantum circuit models.

Linear optical quantum computation, in contrast to non-linear optics, is being encouraged due to the difficulty to experimentally realize large non-linearity required [74]. Linear optics refer to bilinear interaction Hamiltonian in the form of $H = \sum_{jk} A_{jk} \hat{a}_j^\dagger \hat{a}_k$ and the subsequent evolutions. Linear optics Hamiltonians conserve photon numbers, a property that is not satisfied by the general Bogoliubov transformation [75]. Among basic linear optical elements, e.g. half- and quarter-wave plates, phase shifter and etc., beam splitter [76] is mathematically equivalent to other elements and of central importance in QIP. The Hamiltonian of the beam-splitter is given by

$$H_{\mathrm{BS}}(\theta, \phi) = \theta e^{i\phi} \hat{a}_{\mathrm{in}}^\dagger \hat{b}_{\mathrm{in}} + \theta e^{-i\phi} \hat{a}_{\mathrm{in}} \hat{b}_{\mathrm{in}}^\dagger, \tag{4.1}$$

where $\hat{a}_{\mathrm{in}}$ and $\hat{b}_{\mathrm{in}}$ are annihilation operators of two input modes and θ and ϕ are two parameters of the beam splitter, and the action of this Hamiltonian on these

mode is described by the transformation

$$\begin{aligned}\hat{a}^{\dagger}_{\text{out}} &= \cos\theta \hat{a}^{\dagger}_{\text{in}} + ie^{-i\phi}\sin\theta \hat{b}^{\dagger}_{\text{in}}, \\ \hat{b}^{\dagger}_{\text{out}} &= \cos\theta \hat{b}^{\dagger}_{\text{in}} + ie^{-i\phi}\sin\theta \hat{b}^{\dagger}_{\text{in}},\end{aligned} \tag{4.2}$$

where $\hat{a}_{\text{out}}$ and $\hat{b}_{\text{out}}$ are annihilation operators of two output modes.

KLM protocol consists of off-line resources and elementary probabilistic gates, gate teleportation and error correction. Photons interact only via bosonic commutation relation $[\hat{a}, \hat{a}^{\dagger}] = 1$ similarly as in Hong-Ou-Mandel effect [77], and together with projective measurements, probabilistic two-qubit gates can be obtained. Controlled-phase gate (CZ) can be used to construct universal quantum computation [78], and it can be constructed from two nonlinear sign gates (NS) [144] in turn. These gates are written as:

$$\begin{aligned}|q_1, q_2\rangle &\overset{\text{CZ}}{\rightarrow} (-1)^{q_1 q_2} |q_1, q_2\rangle, \\ \alpha|0\rangle + \beta|1\rangle + \gamma|2\rangle &\overset{\text{NS}}{\rightarrow} \alpha|0\rangle + \beta|1\rangle - \gamma|2\rangle,\end{aligned} \tag{4.3}$$

where q_i may take 0 or 1, and $|n\rangle$ are Fock states of photon number n. It should be noted that the above gates cannot work deterministically.

As probabilitic gates can destroy qubits, it is very harmful to QIP, and even may eliminate quantum advantages. In order to circumvent this damage, quantum teleportation may be utilized, in the way that the probabilistic gates act not directly on the qubits but on the prepared resources [17]. In the case of CZ gate which belongs to the Clifford group, application of a few additional Pauli operators to those required for teleportation suffices to achieve this strategy, and

all probabilistic elements are removed in this way.

One critical loop-hole now is that the Bell measurement indispensable for this strategy cannot work deterministically [79, 80], and thus it may seem the original problem cannot be avoided in principle. The resolution discovered by KLM was that not exactly deterministic Bell measurement but nearly deterministic Bell measurement will be a detour, and this can be performed using discrete quantum Fourier transform (cf. [81]), which can be written in matrix notation as

$$(F_n)_{jk} = \frac{1}{\sqrt{n}} \exp[2\pi i \frac{(j-1)(k-1)}{n}], \tag{4.4}$$

where n is the number of mode the Fourier transform acts on, and j and k are matrix indices. Original KLM scheme contrived a teleportation on single-rail qubit (made of a single photon state $|1\rangle$ and a vacuum $|0\rangle$), but there also exists a scheme based on dual-rail qubit (made of a horizontally polarized single photon state $|H\rangle$ and a vertically polarized single photon state $|V\rangle$) [82]. A simple description of KLM teleportation scheme can be summarized as follows. When an input state $|\phi\rangle = \alpha|0\rangle + \beta|1\rangle$ and the 2n-mode entangled state $|t_n\rangle = (n+1)^{-1/2} \sum_{j=0}^{n} |1\rangle^j |0\rangle^{n-j} |0\rangle^j |1\rangle^{n-j}$ is prepared, quantum Fourier transformation F_{n+1} acts on the input state mode and the first n modes of the entangled state, and count the photon number m in these modes. Then the input state $|\phi\rangle$ is teleported into $(n+m)$-th mode in the entangled state modes. An failure occurs when either zero or $n+1$ photons are observed, in which case a collapse occurs onto $|0\rangle$ or $|1\rangle$, and the overall success probability is given as $n/(n+1)$. As the entangled state $|t_n\rangle$ is prepared off-line as a resource, n can be as large as

we want, thus making the overall procedure work near-deterministically.

In order to reduce the amount of resource required, so-called parity encoding was adopted by KLM, where the logical qubit basis is written as:

$$\begin{aligned} |0\rangle_L &= |HH\rangle + |VV\rangle\,, \\ |1\rangle_L &= |HV\rangle + |VH\rangle\,, \end{aligned} \tag{4.5}$$

and can be achieved by a CNOT gate between the original qubit and an ancilla qubit. The purpose of this encoding can be seen as follows. When a measurement is made on one of the physical qubits (which may occur as an error in KLM teleportation procedure), either one of the following transformations takes place:

$$\begin{aligned} \alpha\,|0\rangle_L + \beta\,|1\rangle_L &\to (\alpha\,|H\rangle + \beta\,|V\rangle)\,|H\rangle \\ &\to (\alpha\,|V\rangle + \beta\,|H\rangle)\,|V\rangle\,, \end{aligned} \tag{4.6}$$

where the above (below) corresponds to $|H\rangle$ ($|V\rangle$) detection, and the second case can be corrected by the bit flip gate. As the (corrected) output state $\alpha\,|H\rangle + \beta\,|V\rangle$ can be transformed back to logical encoding by another teleportation through the entanglement such as $|H\rangle\,|0\rangle + |V\rangle\,|1\rangle$, the overall success probability can be raised. KLM boosted the success probability further by concatenation approach, i.e. encoding qubits in the concatenated basis of $|0\rangle_L^{(4)} = |00\rangle_L + |11\rangle_L$ and $|1\rangle_L^{(4)} = |01\rangle_L + |10\rangle_L$. It should be noted at this point that near-deterministic Bell measurement still requires a large resources, and an entangled state such as $|t_n\rangle$ is extremely difficult to experimentally prepare when n is very large.

4.2 Coherent state quantum computation

Another class of qubit encoding strategies using coherent states was proposed [83, 149, 150] due to the above-mentioned difficulty of near-deterministic Bell measurement in the linear optical strategies. Coherent states, an eigenstate of the annihilation operator $\hat{a}\,|\alpha\rangle = \alpha\,|\alpha\rangle$, are considered as a mathematical model of a laser and a state which satisfy the correspondence principle [86]. They have average photon number corresponding to $|\alpha|^2$, and are nonorthogonal to each other, i.e. $\langle\alpha|\beta\rangle \neq 0$. The original proposal [83] adopted the logical qubit basis as equal superpositions of coherent states with equal amplitude in opposite phases, i.e. $|0,1\rangle_L \equiv |\pm\rangle = N_\pm(|\alpha\rangle \pm |-\alpha\rangle)$ where $N_\pm$ is a normalization constant. Another choice is the logical qubit basis as bare coherent states with equal amplitude in opposite phases [149, 150], i.e. $|0,1\rangle_L \equiv |\pm\alpha\rangle$. As they span the same qubit space, there exist no physical difference between those choices. In this thesis, I will adopt the qubit basis as bare coherent states.

Elementary operations using linear optical elements can be constructed in the coherent state architectures, but in a non-deterministic ways due to the non-orthogonality of the basis states. Universal set of quantum gates are constructed with a general single qubit rotation and a two-qubit gate as was pointed before. Arbitrary single qubit rotations can be constructed from two of the three Pauli operators and arbitrary rotation about one axis, and bit-flip gate (X gate) is realized by delaying half a cycle of the local oscillator

$$X = \exp\{i\pi\hat{a}^\dagger\hat{a}\}, \tag{4.7}$$

which works unitarily. Phase rotations about Z-axis are obtained by the action of small imaginary displacement operators $D(i\epsilon) = \exp(i\epsilon\hat{a}^\dagger + i\epsilon\hat{a})$ infinitesimally. A sign-flip gate (Z gate) is achieved by teleportation and application of X gate depending on the Bell measurement outcomes. The principle of this gate is easily shown as the teleportation is equal to identity operation after X- and Z- corrections, thus output state with only X- correction results in Z gate operation for half of the cases (remembering $Z^2 = I$).

The Bell measurement of entangled coherent states [147, 148], the central ingredient among gates of QIP, works quite differently from Fock state basis. Before explaining how this scheme works, it should be mentioned that in precise terms this measurement discriminates between "quasi"-Bell states [89] in the sense that they do not form complete orthogonal basis for bipartite coherent state qubit space. The original proposal works by only using a single beam splitter and a pair of photon number parity detectors. The basic mechanism is that after passing the beam splitter, the quasi-Bell states are transformed as:

$$\begin{aligned} |B_{1,2}\rangle &= N_{1,2}(|\alpha\rangle\,|\alpha\rangle \pm |-\alpha\rangle\,|-\alpha\rangle) \overset{BS}{\to} N_{1,2}(\left|\sqrt{2}\alpha\right\rangle \pm \left|-\sqrt{2}\alpha\right\rangle)\,|0\rangle\,, \\ |B_{3,4}\rangle &= N_{3,4}(|\alpha\rangle\,|-\alpha\rangle \pm |-\alpha\rangle\,|\alpha\rangle) \overset{BS}{\to} N_{3,4}\,|0\rangle\,(\left|\sqrt{2}\alpha\right\rangle \pm \left|-\sqrt{2}\alpha\right\rangle), \end{aligned} \tag{4.8}$$

where N_i's are normalization factors. Now the fact that states $N_\pm(|\beta\rangle \pm |-\beta\rangle)$ have a definite even or odd number of photons depending on the sign can be used. I briefly mention that the two-qubit gates such as CNOT gate is obtained using teleportation through tripartite entanglement such as $|\xi\rangle = N(\left|\sqrt{2}\alpha, \alpha, \alpha\right\rangle + \left|-\sqrt{2}\alpha, -\alpha, -\alpha\right\rangle)$ following the prescription of [17].

One critical drawback of QIP with coherent states is that it is very difficult to generate the superposition of the qubit basis compared to the case of polarization qubit where only a simple rotation of the measurement axis suffices, and no known recipe for generating the coherent state superposition states at arbitrary amplitude in the form of $N(|\alpha\rangle \pm |-\alpha\rangle)$ exists. The recent experimental achievements are an odd superposition with $\alpha \approx 1.6$ [90] using a Fock state with conditioning by homodyne detection after the beam splitter.

Recent progress in the direction of QIP using coherent states is coherent state 3D topological cluster state production using controlled-Z gate [91], a near-deterministic CNOT gate using photon number resolving quantum nondemolition detectors, and feed forward method [153], and implementation of quantum computation using coherent states of the vibrational modes of trapped ions [93]. It was shown recently that smaller resources are required for fault-tolerant quantum computation than single photon schemes [152], thus providing another motivation of using coherent states.

We have to point out as a closing remark of the chapter that there exists a problem of choice of the amplitude of the coherent state qubits as depicted in Fig. 4.1. The difficulty in choosing the amplitude originates from several different tendencies that exist in the coherent state QIP. The fidelities and success probabilities of gate operations such as Z-rotation or that of Bell measurements favor large α's. They grow monotonously to unity as α becomes larger. In contrast, decoherence effect and the experimental generation of coherent state superpositions favor the other direction. There does not exist a generally accepted rule for the choice of coherent amplitude. Recently, a criteria that may help this choice

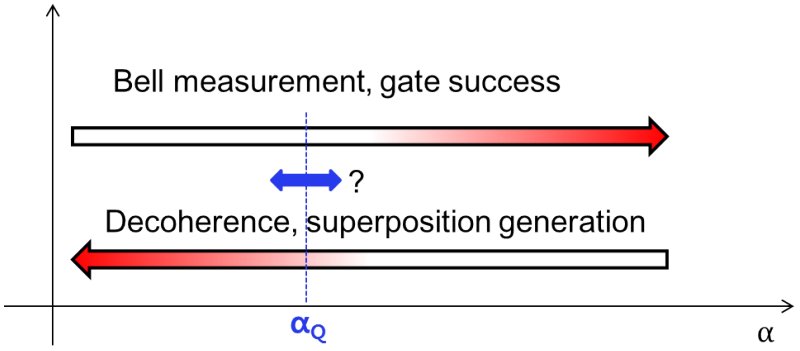

Figure 4.1: The ambiguity of the choice of the coherent amplitude in the coherent state QIP. There exists different tendencies that favors the different limit of α, and it is not trivial to decide which α is the best.

was proposed by Lund *et al.* [152]. In their paper, they showed that the threshold error rate that guarantees fault-tolerance favors $1.2 < \alpha$, and the best choice is about $\alpha \approx 1.5$.

Chapter 5

Entangled Coherent States versus Entangled Photon Pairs for Practical Quantum Information Processing

In this chapter, we will compare effects of decoherence and detection inefficiency on entangled coherent states (ECSs) and entangled photon pairs (EPPs), both of which are known to be particularly useful for quantum information processing (QIP)[1]. When decoherence effects caused by photon losses are heavy, the ECSs outperform the EPPs as quantum channels for teleportation both in fidelities and in success probabilities. On the other hand, when inefficient detectors are used, the teleportation scheme using the ECSs suffers undetected errors that result in the degradation of fidelity, while this is not the case for the teleportation scheme using the EPPs. In this chapter, the merits and demerits of the two types of entangled

[1]This work was published in Phys. Rev. A **82**, 062325 (2010).

states in realizing practical QIP under realistic conditions will be presented. A criteria for the choice of the amplitude of the coherent states is suggested as well with regard to the decoherence effect.

5.1 Introduction

Quantum teleportation uses entangled quantum states as quantum channels, and plays a crucial role in optical quantum computation and communication [144, 17], a prominent candidate for physical implementations of quantum information processing (QIP) [95, 96] as was explained before. One of the most difficult part in realizing quantum teleportation using optical systems is an efficient realization of the Bell-state measurement, as the four Bell states cannot be discriminated when only linear optical elements are used [79, 80]. For example, in the teleportation scheme based on an entangled photon pair (EPP) [97], the success probability of the Bell measurement is bounded by 50% when using only linear optical elements [98]. Even though universal gate operations can be realized based on linear optics and photon detection [144], this type of problem is one of the major hindrances to the implementation of deterministic gate operations as well as scalable quantum computation.

An alternative coherent state qubit-based teleportation scheme was suggested [146, 147] using an entangled coherent state (ECS) as the quantum channel. In fact, the ECSs have been found to be useful not only for fundamental tests of quantum theory [100] but also for various applications in QIP [146, 147, 101, 148, 149, 150, 102, 152, 103, 104]. In this approach, a qubit is composed of two coher-

ent states, $|\pm\alpha\rangle$, where $\pm\alpha$ are the coherent amplitudes [105]. It was explicitly pointed out in Refs. [147, 148] that all the four Bell states in the form of ECSs can be well discriminated using only a beam splitter and two photon-number resolving detectors. This has become a remarkable advantage in designing quantum computing schemes using coherent-state qubits [149, 150] including deterministic gate operations with ECSs as off-line resources [150]. Recently, it was shown that fault-tolerant quantum computing may be realized with coherent-state qubits with amplitudes $\alpha > 1.2$ [152].

Implementations of high-fidelity EPPs and ECSs in free-traveling fields are challenging and crucial tasks for optical QIP. Recently, the realization of an electrically driven source of EPPs, consisting of a quantum dot embedded in a semiconductor light-emitting diode structure, has been reported [106]. Even though the generation of high-fidelity ECSs is a demanding task, remarkable experimental progress has recently been made in generating single-mode superpositions of coherent states [107, 108, 109], with which ECSs would easily be produced using an additional beam splitter. Based on such progress, several suggestions for the same purpose but higher fidelities and larger amplitudes [110] have now become closer to the experimental realization. Efforts to generate arbitrary coherent-state qubits are also being made [111]. Another difficult problem in the approach based on ECSs is that photon number resolving detectors are required, while ongoing efforts are being made for the development of such detectors [112, 113].

Comparing the two optical QIP schemes, one with single photon qubits and EPPs and the other with coherent-state qubits and ECSs, is important as well as interesting for efficient implementations of QIP in the long term. First, deco-

herence of quantum channels caused by photon losses may be an obstacle against optical QIP. This would be non-negligible particularly for long-distance quantum communication, and its effects on the two aforementioned teleportation schemes is studied in this chapter. We found that when decoherence effect caused by photon losses is heavy (or the decoherence time of the quantum channel is long), the ECSs outperform the EPPs as quantum teleportation channels both in teleportation fidelities and in success probabilities. This tendency becomes prominent when the amplitude α is small: the ECSs outperform the EPPs regardless of the decoherence time both in fidelities and in success probabilities for $\alpha \lesssim 0.8$.

The issue of detection inefficiency is another crucial detrimental factor in realizing practical QIP within all-optical systems, and when inefficient detectors are used, the teleportation scheme using ECSs suffers undetected errors that results in the degradation of fidelity. This is not the case for the teleportation scheme using EPPs as photon losses right before the detector errors are detected by the absence of the detection signals itself. We then present the results when both of the two factors, decoherence of the channel and detection inefficiency, are applied. This study based on through quantitative analysis provide useful guidelines for the choice of a scheme among well-known ones for practical QIP using optical systems.

5.2 Decoherence of ECSs and EPPs

In this section, we introduce the dynamics of ECSs and EPPs in a zero-temperature dissipative environment. In this situation, photon losses occur that cause the de-

crease of the average photon number and dephasing of the channels at the same time. We discuss how the degrees of entanglement for the ECSs and EPPs decrease by such decoherence effects.

5.2.1 Solutions of master equation

We are interested in ECSs in the form of [114]

$$|\psi_{\rm ECS}^{\pm}\rangle = N_{\alpha}^{\pm}\left(|\alpha\rangle_1|-\alpha\rangle_2 \pm |-\alpha\rangle_1|\alpha\rangle_2\right), \tag{5.1}$$

where $N_{\alpha}^{\pm} = 1/\sqrt{2 \pm 2e^{-4|\alpha|^2}}$ is the normalization factor. The complex amplitude α is assumed to be real throughout the chapter for simplicity without losing generality. We shall call $|\psi_{\rm ECS}^{+}\rangle$ ($|\psi_{\rm ECS}^{-}\rangle$) even (odd) ECS as it contains only even (odd) numbers of photons, and the sign of the relative phase is even (odd). We also consider an EPP,

$$|\psi_{\rm EPP}\rangle = \frac{1}{\sqrt{2}}\Big(|H\rangle_1|V\rangle_2 + |V\rangle_1|H\rangle_2\Big), \tag{5.2}$$

where $|H\rangle$ and $|V\rangle$ refer to horizontal and vertical polarization states, respectively. The relative sign between the vector components of the EPP in Eq. (5.2) was chosen to be $+1$ for simplicity: this sign does not make any meaningful difference in our study and this is obviously different from the cases of the ECSs in (5.1) for which the signs in the middle play important roles. We also note that $|H\rangle$ is equivalent to $|1\rangle|0\rangle$ and $|V\rangle$ to $|0\rangle|1\rangle$ in terms of the dual-rail logic QIP.

The time evolution of density operator ρ under the Born-Markov approximation is given by the master equation [166] which we derived in the previous

chapter (Eq. (3.12)). Assuming a zero-temperature bath, we obtain the density operator of the odd and even ECSs decohered in the vacuum environment as [147, 146]

$$\begin{aligned}\rho_{\rm ECS}^{\pm}(\tau) =&(N_\alpha^{\pm})^2\Big\{|t\alpha\rangle_1\langle t\alpha|\otimes|-t\alpha\rangle_2\langle -t\alpha|+|-t\alpha\rangle_1\langle -t\alpha|\otimes|t\alpha\rangle_2\langle t\alpha| \\ &\pm e^{-4\alpha^2 r^2}\big(|t\alpha\rangle_1\langle -t\alpha|\otimes|-t\alpha\rangle_2\langle t\alpha|+h.c.\big)\Big\},\end{aligned} \tag{5.3}$$

where $t = e^{-\gamma\tau/2}$ and superscript $+$ $(-)$ corresponds to the even (odd) ECS. We define the normalized time as $r = (1-t^2)^{1/2}$ for later use. In what follows, we shall use only the *odd* ECSs, which are maximally entangled in the $2\otimes 2$ Hilbert space at time $\tau = 0$, as the quantum channels to teleport coherent-state qubits. As we shall explain later, the odd ECS shows larger success probabilities of teleportation than the even ECS. The density matrix $\rho_{\rm ECS}^{-}$ expressed in the orthogonal basis set $|\pm\rangle = N_\pm\big(|t\alpha\rangle \pm |-t\alpha\rangle\big)$ is given as

$$\rho_{\rm ECS}^{-}(\tau) = \frac{1}{4(-1+e^{4\alpha^2})}\begin{pmatrix} A & 0 & 0 & D \\ 0 & B & -B & 0 \\ 0 & -B & B & 0 \\ D & 0 & 0 & C \end{pmatrix}, \tag{5.4}$$

where

$$\begin{aligned} A &= e^{-4(-1+r^2)\alpha^2}(-1+e^{4r^2\alpha^2})(1+e^{2(-1+r^2)\alpha^2})^2, \\ B &= -1+e^{4\alpha^2}-e^{4r^2\alpha^2}+e^{-4(-1+r^2)\alpha^2}, \\ C &= e^{-4(-1+r^2)\alpha^2}(-1+e^{4r^2\alpha^2})(-1+e^{2(-1+r^2)\alpha^2})^2, \\ D &= -1-e^{4\alpha^2}+e^{4r^2\alpha^2}+e^{-4(-1+r^2)\alpha^2}. \end{aligned} \tag{5.5}$$

Using the same master equation, one can also find the density operator of the EPP for general τ, initially given as $\rho_{\mathrm{EPP}}(0) \equiv |\psi_{\mathrm{EPP}}\rangle\langle\psi_{\mathrm{EPP}}|$ at $\tau = 0$,

$$\rho_{\mathrm{EPP}}(\tau) = t^4 \rho_{\mathrm{EPP}}(0) - 2\left(t^4 - t^2\right)\rho_1 + \left(t^4 - 2t^2 + 1\right)\rho_v \tag{5.6}$$

where $\rho_1 = \frac{1}{4}\sum_{i=1}^{4} |1\rangle_i\langle 1|$ is a mixed single photon state density matrix, $|1\rangle_i \equiv |0\rangle \ldots |1\rangle_i \ldots |0\rangle$ is a shorthand notation for a single photon occupying mode i and the vacuum in all other modes, and ρ_v represents the vacuum state for every mode. The density matrix can be represented in a basis set of $|H\rangle$, $|V\rangle$ and $|0\rangle$ similarly as before. As one may expect, in a rough sense, the initial entangled two photon state decays to a mixed single photon state, and then eventually to the vacuum state.

5.2.2 Degrees of entanglement

As quantum teleportation utilizes entanglement as resource, we first consider dynamics of entanglement for the ECSs and EPPs. Separability of a bipartite system is equivalent to the positivity of the partial transpose of the density matrix when the dimension of the entire system does not exceed 6 [39, 116]. We consider the ECSs in a $2 \otimes 2$ Hilbert space (using the dynamic qubit basis) as explained above even under the effect of photon losses. On the other hand, the EPPs evolve into $3 \otimes 3$ systems due to the addition of the vacuum element under photon loss effects. However, in our case of Eq. (5.6), negativity of the total density operator equals the sum of negativities of all the decomposed components. This guarantees from the convexity of the negativity that this decomposition shows the smallest

negativity [117]. It is known that the separability criterion is satisfied in such cases of the "minimum decomposition" [118].

Based on this, the measure of entanglement $E = -2\sum_i \lambda_i^-$ [119] related to the aforementioned negativity can be used, where λ_i^- are negative eigenvalues of the partial transpose of the density operator. Using Eqs. (5.4), (5.5) and the above-mentioned definition of the entanglement measure, the degree of entanglement for an odd ECS is obtained as

$$E_{\mathrm{ECS}}(\alpha, r) = -\frac{A + C - \sqrt{A^2 + 4B^2 - 2AC + C^2}}{4(-1 + e^{4\alpha^2})}, \tag{5.7}$$

and the degree of entanglement for the EPP is

$$E_{\mathrm{EPP}}(r) = (1 - r^2)^2. \tag{5.8}$$

We have plotted the degrees of entanglement for the EPPs and ECSs for several values of α in Fig. 5.1. As it is already discussed [119, 120] the ECSs with large amplitudes decohere faster than those with small amplitudes. In the limit of $\alpha \to 0$, it is straightforward to show that

$$E_{\mathrm{ECS}}(\alpha, r) = -r^2 + \sqrt{1 - 2r^2 + 2r^4} < E_{\mathrm{EPP}}(r) \tag{5.9}$$

for $0 < r < 1$. Obviously, the EPP is always more entangled than the ECS for any values of α.

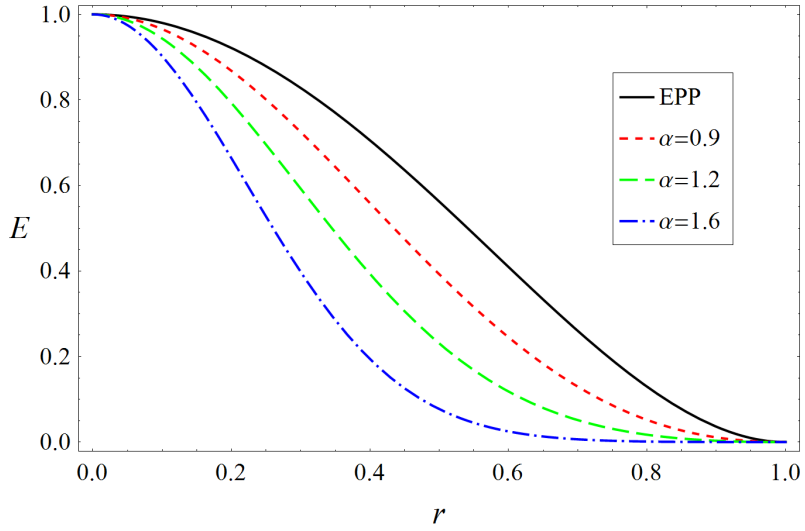

Figure 5.1: Degrees of entanglement E against the normalized time r. The EPP shows larger entanglement than ECSs at any time regardless of α [169].

5.3 Teleportation with ECS and EPP

It is obvious that with quantum channels decohered for non-zero decay time, teleportation fidelities will degrade. This effect should not be neglected particularly for long-distance quantum teleportation. Detection inefficiency may be an even more crucial factor when considering practical quantum teleportation using optical systems. It is often considered as photon losses in front of ideal detectors. We also note that dark count rates may be non-negligible for the cases of highly efficient detectors such as photon number resolving detectors necessary for the teleportation using the ECS. In this section, we thoroughly analyze the first two degrading factors due to photon losses as depicted in Fig. 5.2.

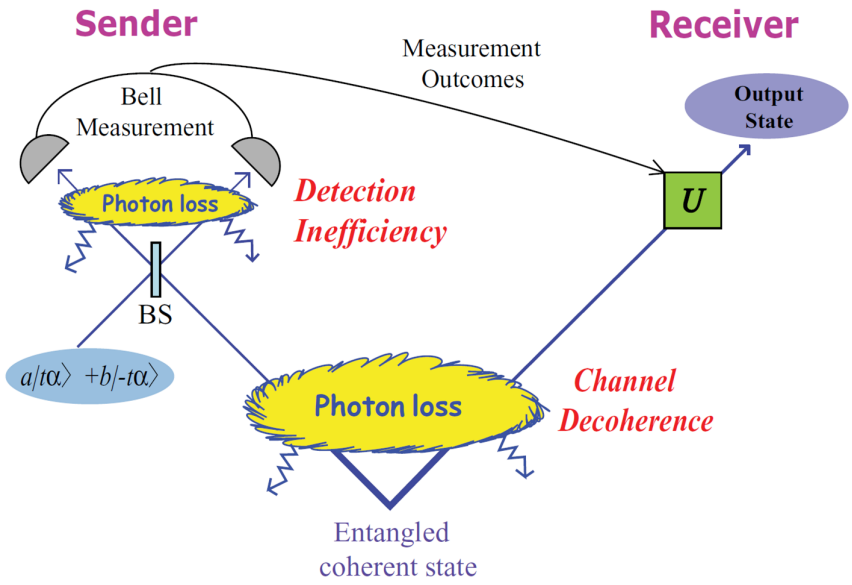

Figure 5.2: Teleportation protocol using the ECS with two kinds of "photon losses." Photon losses during the propagation of the quantum channel cause the "channel decoherence" while photon losses before ideal detectors are introduced to model detection inefficiency. BS represents a 50:50 beam splitter and U the unitary operation required to restore the input state [169].

5.3.1 Effects of channel decoherence

The fidelity F between input and output states for quantum teleportation is defined as $F = \langle\phi_{\rm in}|\rho_{\rm out}|\phi_{\rm in}\rangle$, where $|\phi_{\rm in}\rangle$ is the input state and $\rho_{\rm out}$ is the density operator of the output state. For the case of an ECS, one can use $|t\alpha\rangle$ and $|-t\alpha\rangle$ as a dynamic qubit basis in order to reflect amplitude losses as suggested in Ref. [147]. Then an unknown qubit reads

$$|\phi_{\rm in}\rangle = a|t\alpha\rangle + b|-t\alpha\rangle, \tag{5.10}$$

where a and b are arbitrary complex numbers under the normalization condition. The basis states $|t\alpha\rangle$ and $|-t\alpha\rangle$ are not orthogonal, but they approach such the limit for $t\alpha \gg 1$. One can construct an orthogonal basis, $|\pm\rangle = n_{\pm}(|t\alpha\rangle \pm |-t\alpha\rangle)$ with normalization factors $n_{\pm}$, using their linear superpositions [121]. In this way, one can consider the qubit (channel) in a 2-dimensional ($2 \otimes 2$-dimensional) Hilbert space even under the decoherence effects. The input state can also be expressed as

$$|\phi_{\rm in}\rangle = \cos(u/2)e^{{\rm i}\frac{v}{2}}|+\rangle + \sin(u/2)e^{-{\rm i}\frac{v}{2}}|-\rangle. \tag{5.11}$$

The coefficient u and v are related to a and b as

$$\begin{aligned} a &= n_+ \cos(u/2)e^{{\rm i}\frac{v}{2}} + n_- \sin(u/2)e^{-{\rm i}\frac{v}{2}}, \\ b &= n_+ \cos(u/2)e^{{\rm i}\frac{v}{2}} - n_- \sin(u/2)e^{-{\rm i}\frac{v}{2}}. \end{aligned} \tag{5.12}$$

The initial total state is then represented as

$$\rho^{\rm tot} = |\phi_{\rm in}\rangle_A\langle\phi_{\rm in}| \otimes \{\rho_{\rm ECS}(\tau)\}_{BC}, \tag{5.13}$$

where A and B are modes for the sender while C is for the receiver. In order to discriminate between the Bell states, a 50:50 beam splitter for modes A and B is used. We here define the beam splitter operator as

$$U_{i,j}(\theta) = e^{-\frac{\theta}{2}(a_i^\dagger a_j - a_i a_j^\dagger)}, \tag{5.14}$$

where i and j are two field modes entering the beam splitter, and θ is related to the transmittivity $\zeta = \cos^2(\theta/2)$. The action of the 50:50 beam splitter, $U_{A,B}(\pi/2)$, may be characterized as $U_{A,B}(\pi/2)|\alpha\rangle_A|\beta\rangle_B = |(\alpha+\beta)/\sqrt{2}\rangle_A|(-\alpha+\beta)/\sqrt{2}\rangle_B$. The Bell states with coherent states in our context are

$$|\Phi^\pm\rangle = N_\pm(|t\alpha\rangle_1|t\alpha\rangle_2 \pm |-t\alpha\rangle_1|-t\alpha\rangle_2), \tag{5.15}$$

$$|\Psi^\pm\rangle = N_\pm(|t\alpha\rangle_1|-t\alpha\rangle_2 \pm |-t\alpha\rangle_1|t\alpha\rangle_2), \tag{5.16}$$

where $N_\pm$ are normalization factors. After the action of the beam splitter, two photon number resolving detectors are required for modes A and B to complete the Bell-state measurement [147]. The projection operators O_j for the outcomes

j representing the parity measurement can be written as

$$O_1 = \sum_{n=1}^{\infty} |2n\rangle_A\langle 2n| \otimes |0\rangle_B\langle 0|, \tag{5.17}$$

$$O_2 = \sum_{n=1}^{\infty} |2n-1\rangle_A\langle 2n-1| \otimes |0\rangle_B\langle 0|, \tag{5.18}$$

$$O_3 = \sum_{n=1}^{\infty} |0\rangle_A\langle 0| \otimes |2n\rangle_B\langle 2n|, \tag{5.19}$$

$$O_4 = \sum_{n=1}^{\infty} |0\rangle_A\langle 0| \otimes |2n-1\rangle_B\langle 2n-1|, \tag{5.20}$$

where we refer to Φ^+, Φ^-, Ψ^+ and Ψ^- as subscripts (or superscripts) 1, 2, 3 and 4 for simplicity. In addition to the operators in Eqs. (6.23-6.26), the error projection operator, $O_{\rm e} = |0\rangle_A\langle 0| \otimes |0\rangle_B\langle 0|$, should also be considered because there is possibility for both the detectors not to register anything even though such probability is very small when α is reasonably large.

The unnormalized state after measurement outcome j is obtained as

$$\rho^j = {\rm Tr}_{AB}[U_{A,B}(\pi/2)\rho_{\rm tot}U^\dagger_{A,B}(\pi/2)O_j]. \tag{5.21}$$

Depending on the outcomes of the Bell-state measurement, different unitary rotations on the coherent-state qubit for mode C are required. Applying an appropriate unitary operation U_j which corresponds to X gate in [150] for $j = 2$ and no operation for $j = 4$, the unnormalized output state is obtained as $\rho^j_{\rm out} = U_j\rho^j U^\dagger_j$. While no transformation or only a simple phase shifter is required for the cases of Ψ^- and Φ^-, the displacement operator is required for the other two cases that degrades the fidelity when α is small. We simply exclude such "fidelity-degrading"

cases in this chapter as the success probability with an ECS is always higher than that with an EPP even *without* those cases.

We find for the case of Ψ^-

$$\begin{aligned} p_4 f_4 &= \langle \phi_{\rm in} | \rho^4_{\rm out} | \phi_{\rm in} \rangle \\ &= (N^-_\alpha)^2 e^{-2t^2\alpha^2} \sinh(2t^2\alpha^2) \\ &\Big[|b|^2 |a e^{-2t^2\alpha^2} + b|^2 + |a|^2 |a + b e^{-2t^2\alpha^2}|^2 \\ &+ e^{-4\alpha^2(1-t^2)} a^* b (a^* e^{-2t^2\alpha^2} + b^*)(a + b e^{-2t^2\alpha^2}) + h.c. \Big] \\ &= p_2 f_2, \end{aligned} \tag{5.22}$$

where $p_j = {\rm Tr}(\rho^j_{\rm out})$ is the probability of measuring a particular outcome j and f_j is the teleportation fidelity with that outcome. The success probability p_4 for Φ_- is obtained as

$$\begin{aligned} p_4 = {\rm Tr}(\rho^4_{\rm out}) &= (N^-_\alpha)^2 e^{-2t^2\alpha^2} \sinh(2t^2\alpha^2) \Big[|a|^2 + |b|^2 + e^{-4\alpha^2(1-t^2)} e^{-2t^2\alpha^2} (a^* b + a b^*) \Big] \\ &= p_2. \end{aligned} \tag{5.23}$$

The same calculations can be performed for the case of Ψ_-, which results in the same fidelity and the success probability. The average teleportation fidelity over all unknown input states and the success probability are

$$F_{\rm av} = \frac{1}{4\pi} \int_0^\pi {\rm d}u \sin u \int_0^{2\pi} {\rm d}v \frac{\sum_j p_j f_j}{\sum_j p_j}, \tag{5.24}$$

$$P = \frac{1}{4\pi} \int_0^\pi {\rm d}u \sin u \int_0^{2\pi} {\rm d}v \sum_j p_j, \tag{5.25}$$

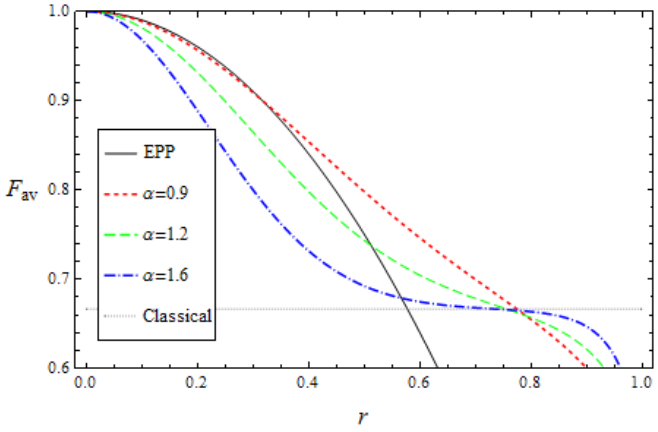

Figure 5.3: The average teleportation fidelities, F_{av}, of the ECSs and the EPP as quantum channels against the normalized time r. The dotted horizontal line indicates the maximum classical limit, 2/3, which can be achieved by classical means [169].

where the summations run over only 2 and 4 since we discard all the other cases. One can show by performing the integration in (5.25) that the average success probability for the ECS is $P_{\text{ECS}} = 1/2$, regardless of α. As we perform the integration in (5.24), we obtain the expression

$$F_{\text{ECS}}(\alpha, r) = 2n\frac{l-m}{c} + 2n\frac{d^2(l-m)+2c^2m}{c^3}\frac{\text{arctanh } d/c - d/c}{(d/c)^3}, \tag{5.26}$$

where now $l = 3e^{8\alpha^2} - 5e^{4\alpha^2(r^2+1)} + 5e^{4\alpha^2(2+r^2)} - 3e^{4\alpha^2(1+2r^2)}$, $m = (e^{4\alpha^2} + e^{4r^2\alpha^2})(e^{4\alpha^2} - e^{4\alpha^2(1+r^2)})$, $n = e^{-4\alpha^2(1+r^2)}/16$, $c = e^{4\alpha^2} - 1$ and $d = -e^{2(1+r^2)\alpha^2} + e^{-2(-1+r^2)\alpha^2}$. We have plotted the results in Fig. 5.3.

The calculations are straightforward for the case of the EPP because of the orthogonal nature of the qubit and the channel. In this case, only two ($|\Psi'^{+}\rangle$ and $|\Psi'^{-}\rangle$) among the four Bell states, $|\Phi'^{\pm}\rangle = (|H\rangle_1|H\rangle_2 \pm |V\rangle_1|V\rangle_2)/\sqrt{2}$ and

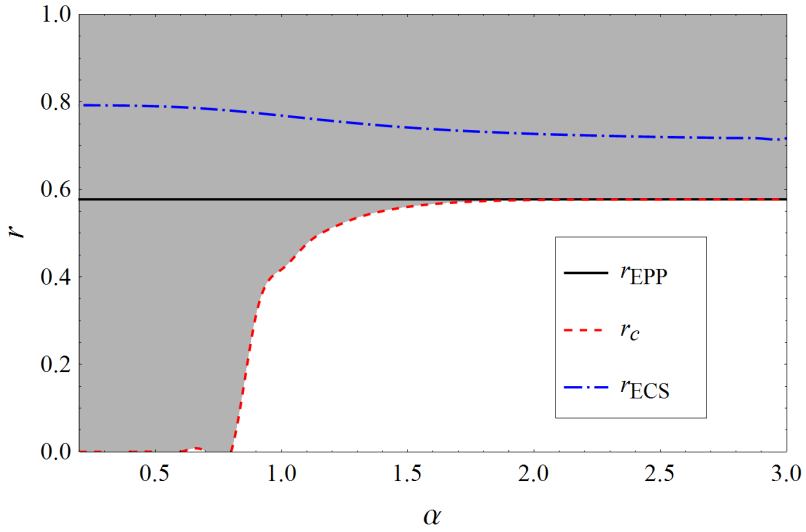

Figure 5.4: The average fidelity using the EPP falls below the classical limit at r_{EPP} (solid line). The average fidelity using the ECS, F_{ECS}, becomes larger than that using the EPP, F_{EPP}, at time r_{c} and falls below the classical limit at r_{ECS}. The grey shaded area corresponds to $F_{\mathrm{ECS}} > F_{\mathrm{EPP}}$ [169].

$|\Psi'^{\pm}\rangle = (|H\rangle_1|V\rangle_2 \pm |V\rangle_1|H\rangle_2)/\sqrt{2}$, can be identified using linear optics elements and photodetectors. This means that the success probability cannot exceed 1/2 [80]. The average fidelity and the success probability can easily be obtained in the same manner explained above as $F_{\rm EPP}(r) = 1 - r^2$ and $P_{\rm EPP} = (1 - r^2)/2$, respectively. Here, it is immediately clear that $P_{\rm ECS} = 1/2 > P_{\rm EPP}$: the success probability using the ECS is higher than that using the EPP regardless of α.

In Fig. 5.3, the average fidelities for the ECS and the EPP, $F_{\rm ECS}$ and $F_{\rm EPP}$ respectively, are plotted and compared. The classical limit denoted by the horizontal dotted line in the figure is 2/3, under which quantum channels become useless for teleportation of qubits. We find that the teleportation fidelities using the ECSs stay above the classical limit longer than those with the EPP regardless of the values of α. As shown in Fig. 5.3, the EPP becomes useless for teleportation at time $r_{\rm EPP} = 1/\sqrt{3} \approx 0.577$ while the ECSs become useless at $r_{\rm ECS}$, where $r_{\rm ECS}$ is determined between 0.7 and 0.8 depending on α. We have investigated the cases for large values of α up to 4, and our numerical results lead us to conjecture that $r_{\rm ECS}$ converges to ~ 0.7 when α becomes large. As shown in Fig. 5.4, $F_{\rm ECS}$ remains lower than $F_{\rm EPP}$ until the decoherence time r becomes r_c. When the decoherence time reaches r_c, $F_{\rm ECS}$ exceeds $F_{\rm EPP}$. Of course, $F_{\rm ECS}$ eventually falls below the classical limit at time $r_{\rm ECS}$ as we mentioned above. Remarkably, $r_{\rm c} \approx 0$ for $\alpha \lesssim 0.8$, which means that the ECSs outperform the EPP for these values of α.

Even though the EPP is always more entangled than ECS (Fig. 5.1), it does not always mean higher teleportation fidelity (Fig. 5.3). The reason for this can be understood as originated from the different dynamics of the two channels

under photon loss effects. With the ECS channels, we have been able to minimize the degradation of the teleportation fidelity using the dynamic qubit basis [147]. This is not possible with the EPP. Photon losses cause the EPP to have the "vacuum" elements both at the sender's mode and at receiver's. In other words, the decohered EPP gets out of the initial $2 \otimes 2$ Hilbert space composed of $|H\rangle$ and $|V\rangle$ and this "escape" for the EPP is a major difference from the case of the ECS. The vacuum portion at receiver's mode, C, results in a significant decrease of the teleportation fidelity. (On the contrary, in the following subsection, it becomes clear that the vacuum elements at sender's modes, A and B, are noticed by a failure of the Bell-state measurement and such an error can be discarded so that the fidelity is not affected.)

We here comment on the difference between the previous result in Ref. [147] and ours in this thesis. In Ref. [147], the time r at which the teleportation fidelity of the ECS falls below the classical limit was independent of α. In that paper, the singlet fraction of the channel state was used to calculate the optimal teleportation fidelity by the method suggested in Ref. [122]. However, this method is not optimized for the ECS under our decoherence model based on photon losses: when ρ^{-}_{ECS} is partially traced over one of the modes, the reduced density matrix is not proportional to the identity matrix, which is the condition required to apply the singlet fraction method presented in Ref. [122].

So far, we have not considered the even ECS. Because of the same reason as the case of the odd ECS, only ψ^{+} and ϕ^{+} can be considered the successful Bell measurement results. For the results with the even ECS, the teleportation fidelity becomes identical to the case of the odd ECS. However, the success prob-

ability is lower than that of the odd ECS according to our calculation for the same value of α. The reason for this is as follows. We utilize the results of odd photon detection for the case of the odd ECS, while the results of the non-zero even photon detection, corresponding to ψ^+ and ϕ^+, are used for the case of the even ECS. The odd photon detection probability is the same to the even photon detection probability when taking the average over all input states. However, the even photon detection probability contains the "all-zero" cases, which are eventually discarded, and this inconclusive failure probability gets larger as the amplitude becomes smaller. Therefore, the even ECS channel results in lower success probability unless $\alpha \to \infty$.

5.3.2 Effects of detection inefficiency

We now consider the inefficiency of detectors that is one of the major obstacles to the realization of quantum teleportation using optical systems. An inefficient detector can be modeled by inserting a beam splitter of transmittivity η in front of the perfect detector, where the beam splitter operation mixing the light with fictitious vacuum mode can be denoted as $U^{\eta}_{i,j} \equiv U_{i,j}(\theta_\eta)$ where $\theta_\eta = 2\cos^{-1}\sqrt{\eta}$, where i and j are indices for modes. In order to perform the Bell-state measurement, we first need to apply the 50:50 beam splitter to the total density operator $\rho^{\rm tot}$ in Eq. (5.13). The beam splitter operations, U^{η}, for inefficient detectors are then applied to incorporate detection inefficiency. The resultant density operator after tracing out the irrelevant vacuum modes (v_1 and v_2) is

$$(\rho^{\eta})_{\rm ABC} = {\rm Tr}_{v_1,v_2}\Big[\mathbb{U}\{(\rho^{\rm tot})_{ABC} \otimes (|0\rangle\langle 0|)_{v_1} \otimes (|0\rangle\langle 0|)_{v_2}\}\mathbb{U}^{\dagger}\Big], \tag{5.27}$$

where $\mathbb{U} = U^{\eta}_{A,v_1} U^{\eta}_{B,v_2} U_{A,B}(\pi/2)$ is the total unitary operation including the action of both the physical and virtual beam splitters. The unnormalized density matrix for measurement outcome j is given as $\rho^{j}_{out} = U_j[Tr_{AB}(\rho^{\eta} O_j)]U_j^{\dagger}$. Using Eqs. (5.18) and (6.26), we find

$$p_2 f_2 = p_4 f_4 = \langle \psi_{in} | \rho^4_{out} | \psi_{in} \rangle = D(N^-_{\alpha})^2 \Big[|L|^2 + |M|^2 + 2e^{-4\alpha^2 r^2} C^2 Re(M^* L) \Big] \tag{5.28}$$

and the probability for each outcome is given as

$$p_2 = p_4 = Tr(\rho^4_{out}) = D(N^-_{\alpha})^2 \Big[|a|^2 + |b|^2 + 2e^{-2\alpha^2(1+r^2)} C^2 Re(a^* b) \Big], \tag{5.29}$$

where $D = e^{-2\eta(1-r^2)\alpha^2} \sinh\left(2\eta(1-r^2)\alpha^2\right)$, $C = e^{-2(1-r^2)\alpha^2(1-\eta)}$, $M = a^*(a + be^{-2(1-r^2)\alpha^2})$ and $L = b^*(ae^{-2(1-r^2)\alpha^2} + b)$, and the average fidelity is obtained using Eq. (5.24) as

$$F_{\mathrm{ECS}}(\eta, \alpha, r) = 2n \frac{l-m}{c} + 2n \frac{d^2(l-m) + 2c^2 m}{c^3} \frac{\operatorname{arctanh}\, d/c - d/c}{(d/c)^3}, \tag{5.30}$$

where now $l = 3S^{2(1+\eta)} - 5S^{2(r^2+\eta)} + 5S^{2(2+r^2\eta)} - 3S^{2(1+r^2(1+\eta))}$, $m = (S^2 + S^{2r^2})(S^{2\eta} - S^{2(1+r^2\eta)})$, $n = S^{-2(1+r^2\eta)}/16$, $c = S^2 - S^{-2(-1+r^2)(-1+\eta)}$, $d = -S^{(1+r^2)} + S^{-(-1+r^2)(-1+2\eta)}$, and $S = \langle \alpha | -\alpha \rangle = e^{-2\alpha^2}$ is the overlap between coherent states.

We first plot the teleportation fidelities for $r = 0$ (i.e. without decoherence) in Fig. 5.5(a). It is clear that the ECSs with larger amplitudes are more sensitive to inefficiency of the detectors (i.e. decrease of η). The reason for this is similar to the case of the channel decoherence. The action of the beam splitter used for

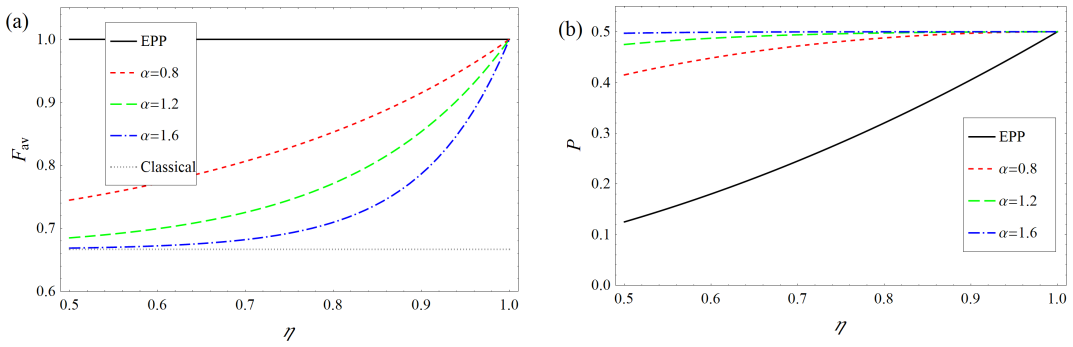

Figure 5.5: (a) Teleportation fidelities using the ECS and the EPP as quantum channels in terms of the efficiency η of detectors. The ECS with large α shows smaller fidelity than that with small α while the fidelity using the EPP is not affected η. (b) The success probabilities of teleportation using the ECS and EPP. The success probability of the EPP decreases faster than that of the ECS by η. Decoherence of the channels is not considered to clearly see the effect of the detection inefficiency [169].

the Bell-state measurement may be described as

$$\begin{aligned}(a|\alpha\rangle + b|-\alpha\rangle)|\alpha\rangle &\rightarrow a|\sqrt{2}\alpha\rangle|0\rangle + b|0\rangle|\sqrt{2}\alpha\rangle,\\ (a|\alpha\rangle + b|-\alpha\rangle)|-\alpha\rangle &\rightarrow a|0\rangle|-\sqrt{2}\alpha\rangle + b|-\sqrt{2}\alpha\rangle|0\rangle.\end{aligned} \tag{5.31}$$

It is then obvious that there are, for example, "cross" terms such as $|\pm\sqrt{2}\alpha\rangle\langle\mp\sqrt{2}\alpha|$ as well as the "diagonal" terms such as $|\pm\sqrt{2}\alpha\rangle\langle\pm\sqrt{2}\alpha|$ before the detection. Then, the cross terms described above in the density matrix are reduced as $\propto e^{-4(1-\eta)\alpha^2}|\pm\sqrt{\eta}\sqrt{2}\alpha\rangle\langle\mp\sqrt{\eta}\sqrt{2}\alpha|$ while the diagonal terms change simply to $\propto |\sqrt{\eta}\sqrt{2}\alpha\rangle\langle\sqrt{\eta}\sqrt{2}\alpha|$ due to photon losses modeled by beam splitters right in front of the "perfect" detectors. It is then straightforward to see that this reduction of the cross terms eventually causes the teleported qubit to be mixed. Therefore, the inefficiency of the detectors (modeled by the additional beam split-

ters) causes the teleported qubit to be "more mixed" when when the amplitude is larger.

On the contrary, the detection efficiency does not affect the teleportation fidelity using the EPP. In this case, the number of photons that should be registered by the Bell measurement is precisely defined as two. The Bell measurement succeeds only when two photons are registered by two of the four detectors used for the measurement [80]. If photon loss occurs due to the inefficiency of the detectors so that only one photon (or no photon at all) is detected, it will be immediately recognized by Alice as a failure. Alice can then simply filter out this kind of "detected" errors to prevent the decrease of the fidelity.

The success probability of teleportation using the ECS is obtained by Eq. (5.25), p_2 and p_4 in Eq. (5.29) as:

$$\begin{aligned} P_{\mathrm{ECS}}(\eta,\alpha,r) =& \frac{1}{4} S^{-2(-1+r^2)(-1+\eta)}(-1+S^{2(-1+r^2)\eta}) \\ & (-1+S^{2(1+(-1+r^2)(-1+\eta))})(-1+S^2)^{-1} \\ & (-1+S^{2(-1+r^2)})^{-1}. \end{aligned} \tag{5.32}$$

The ECSs with small α show lower success probabilities than large α as seen in Fig 5.5(b). When α is small, even a small amount of photon losses may significantly increase the possibility of O_e (i.e., silence of both the detectors), while this is not the case for large α. Therefore, the success probability using the ECSs with small α is more sensitive to detection inefficiency, which is opposite to the case of the fidelity.

Of course, the "filtering out" of the detected errors for the case of the EPP

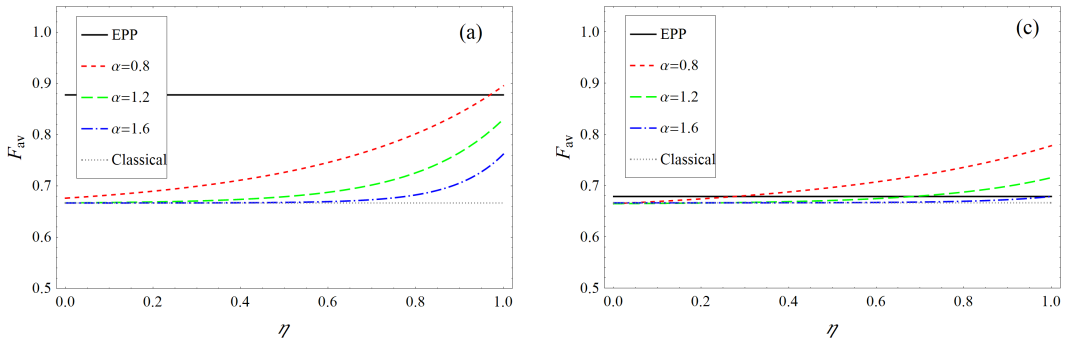

Figure 5.6: Teleportation fidelities against detection efficiency η at decoherence time (a) $r = 0.35$ and (b) $r = 0.566$ for several values of α. As r becomes larger, the fidelity with the EPP drops more rapidly than the fidelities with the ECS [169].

results in the more rapid decrease of the success probability. The success probability using the EPP including the inefficient detector is similarly obtained as for the case of the ECS as

$$P_{\mathrm{EPP}}(\eta, r) = \frac{1 - r^2}{2}\eta^2 \tag{5.33}$$

and is plotted in Fig. 5.5(b). The additional factor η^2 when compared to the probability for the perfect detection case means that each of the two photons in the Bell-measurement module is successfully detected with probability η. Here, we can easily check that the success probability of the ECS is larger than the EPP regardless of α, r and η. Eq. (5.32) is reduced to $(2\eta + r^2(-1+\eta)\eta - \eta^2)/2$ when $\alpha \to 0$, and cannot be smaller than $P_{\mathrm{EPP}}(\eta, r)$ for any η and r.

5.3.3 Photon losses both in channels and at detectors

So far, we have separately considered two different kinds of photon losses, the losses in the channel (referred to as channel decoherence) and the losses at the

detectors (detection inefficiency) used for the Bell-state measurements. In realistic situations, both kinds of losses exist, and it is meaningful to know how the fidelities change under the combination of these effects.

If the ECS shows larger fidelity than the EPP with the perfect detector, it is expected that this is true with imperfect detectors for some moderate values of η. As shown in Fig. 5.6, the ECSs begin to show larger fidelities even with inefficient detectors as the decoherence time gets larger. As noted in the previous section, only the channel decoherence degrades the teleportation fidelity with the EPP, while the teleportation fidelity with the ECS is affected by both the channel decoherence and the detection inefficiency. When the decoherence effect is as dominant as $r > 0.577$, the teleportation fidelity with EPP becomes lower than the classical limit, 2/3, and the teleportation fidelities with the ECSs are always higher regardless of any other conditions.

5.4 Remarks

In this chapter, our attempt was to compare ECSs and EPPs as resources for QIP under realistic conditions. We have considered decoherence caused by photon losses in ECSs and EPPs as quantum channels for teleportation. We have pointed out that entanglement of the EPPs is always larger than that of the ECSs in a dissipative environment. On the other hand, the ECSs outperform the EPPs for the standard teleportation protocol in fidelities for $\alpha \lesssim 0.8$. Furthermore, the success probabilities for teleportation using the ECSs are always higher than those using the EPPs. However, as α gets larger, the range for which the EPPs

show higher fidelities appears.

In general, teleportation fidelity using the ECSs remains over the classical limit longer than that of the EPPs. In other words, even when the EPPs become useless for teleportation due to significant decoherence effects, the ECSs can still be useful for the same purpose. Based on our numerical results we would conjecture that the ECSs are useful for teleportation until the normalized time becomes $r \approx 0.7$ regardless of α while the EPPs become useless when $r \approx 0.577$. However, when α is too large as, e.g., $\alpha > 1.6$, this fidelity merit of the ECSs is too tiny so as to make the teleportation process useless. We have thus pointed out that the degrees of decoherence in the quantum channels are a crucial factor to decide whether the ECSs or the EPPs should be used for efficient QIP. On the other hand, it should be noted that the requirement for fault tolerant quantum computing using coherent-state qubits is very demanding [152].

We also pay special attention to detection inefficiency that is a crucial detrimental factor in realizing practical QIP using all-optical systems. We point out that when inefficient detectors are used for Bell-state measurements, the teleportation scheme using the ECSs suffers undetected errors that result in the degradation of fidelity. This is not the case for the teleportation scheme using the EPPs as photon losses right before the detector are noticed by the absence of the detection signals itself. Finally, we have presented analytical results and examples when both the channel decoherence and detection inefficiency are considered. Our results based on a through quantitative analysis reveal the merits and demerits of the two types of entangled states in realizing practical QIP under realistic conditions, and provide useful guidelines for the choice among the well-known QIP

schemes based on optical systems.

Chapter 6

Quantum Teleportation between Particle-like and Field-like Qubits under Decoherence

Quantum teleportation can act as an interface (e.g. VI. of [123]) between different QIP schemes to overcome difficulties of individual ones. We will analyze quantum teleportation between two different types of optical qubits, one of which is a particle-like and the other is a field-like qubit, under the effect of decoherence. Photon polarization is chosen as the basis of particle-like qubit, while coherent state or photon Fock state is of the field-like qubit. A hybrid entangled state of two different types of qubits is used as the teleportation channel. The teleportation fidelity and success probability are investigated for different channels, and their tendencies are discussed in terms of the effects of decoherence and the physical differences of input and output qubits. It is shown that the teleportation from particle-like to field-like qubits can be achieved with a higher fidelity than the

teleportation in the opposite direction.

6.1 Introduction

In optical implementations of quantum information processing (QIP), some physical degrees of freedom of light are used for qubit encoding [141, 142, 143]. For example, horizontal and vertical polarization states $|H\rangle$ and $|V\rangle$ of a single photon may be used to form a qubit basis. This type of encoding is referred to as *particle-like* encoding [143] as individual photons are information carriers. It is also called dual-rail encoding as it uses two distinct optical modes for a qubit [144]. In this type of approach, single-qubit gates can be easily realized using linear optics elements, while two-qubit operations are generally difficult to implement. Alternatively, one may encode information into two distinct states of a field mode such as the vacuum and single photon [145] or two coherent states of distinct amplitudes [149, 150, 151]. This type of encoding is called *field-like* encoding (or single-rail encoding) [143]. The coherent state encoding has advantages for the Bell-state measurement [147, 148], and quantum computation schemes [149, 150] based on its distinctive teleportation method [146, 147] have been developed. Each of the two encoding schemes has its own advantages and disadvantages for QIP [152].

There have been studies on QIP based on hybrid structures using both particle-like and field-like features of light [153, 154, 155, 156, 157, 158, 159]. This type of "hybrid architecture" may be used to make up for the weaknesses in both type of qubit structures. Indeed, a near-deterministic universal quantum computation

with relatively a small number resources is found to be possible using linear optics with a hybrid qubit composed of photon polarization and coherent state [159]. In this regard, it is important to fully investigate such hybrid architectures, and information transfer between different types of qubits would be a crucial task. The quantum teleportation protocol [160] can be used for such information transfer from one type of system to another. For example, Ralph *et al.* discussed a scheme to perform teleportation between a dual rail (polarization) and single rail (vacuum and single photon) qubits [161]. In addition, in order to address practical conditions for such information transfer, it would also be important to include decoherence effects caused by photon losses that are typical in optical systems.

In this chapter, we study quantum teleportation between particle-like and field-like qubits under decoherence effects. We first consider teleportation between polarization and coherent-state qubits, and that between a polarization qubit and a qubit of the vacuum and single photon. In our study, in general, teleportation from particle-like to field-like qubits shows higher fidelities under decoherence effects compared to teleportation in the opposite direction. However, teleportation from field-like to particle-like qubits is, in general, more efficient in terms of the success probabilities. This implies that the "direction" of teleportation should be considered to be an important factor when developing optical hybrid architectures for QIP.

This chapter is organized as follows. In Sec. 6.2, the time evolution of the two hybrid entangled states under photon losses is investigated. The degrees of entanglement for the hybrid channels are calculated in Sec. 6.3. The average fidelities and success probabilities of teleportation are in Secs. 6.4 and 6.5. Sec. 6.4

deals with teleportation between polarization and coherent-state qubits while Sec. 6.5 is devoted to investigate teleportation between polarization and single-rail Fock state qubits. An exemplary strategy to use these hybrid channels in beneficial ways is presented in Sec. 6.6. We conclude the chapter with final remarks in Sec. 6.7.

6.2 Time evolution of teleportation channels

The first kind of teleportation channel considered in this chapter is a hybrid entangled state of the photon polarization and coherent state:

$$|\psi_{pc}\rangle = \frac{1}{\sqrt{2}}\Big(|H\rangle_p |\alpha\rangle_c + |V\rangle_p |-\alpha\rangle_c \Big), \tag{6.1}$$

where $|\pm\alpha\rangle$ are coherent states of amplitudes $\pm\alpha$. We assume that α is real for simplicity throughout the chapter without loss of generality. The other one is a hybrid channel of the photon polarization and the single-rail photonic qubit

$$|\psi_{ps}\rangle = \frac{1}{\sqrt{2}}\Big(|H\rangle_p |0\rangle_s + |V\rangle_p |1\rangle_s \Big), \tag{6.2}$$

where $|0\rangle$ and $|1\rangle$ denote the vacuum and the single photon state in the Fock basis, respectively, comprising a field-like (single-rail) qubit. Here, p, c and s respectively stand for polarization, coherent state and single-rail Fock state qubits. It is known that hybrid channel $|\psi_{pc}\rangle$ can in principle be produced using a weak cross-Kerr nonlinear interaction between a polarization (dual-rail) single photon qubit and a coherent state [162, 153, 155]. However, it is highly challenging to perform the required nonlinear interaction with high efficiency [163, 164, 165]. The hybrid

channel $|\psi_{ps}\rangle$ can be generated using a parametric down conversion, a Bell state measurement with polarization qubits and an adaptive measurement [161].

We consider decoherence caused by photon loss (dissipation) on the teleportation channels. The dissipation for state ρ is described by the master equation under the Born-Markov approximation with zero temperature environment [166]

$$\frac{\partial \rho}{\partial \tau} = \hat{J}\rho + \hat{L}\rho, \tag{6.3}$$

where τ is the system-bath interaction time. Lindblad superoperators $\hat{J}$ and $\hat{L}$ are defined as $\hat{J}\rho = \gamma \sum_i a_i \rho a_i^\dagger$ and $\hat{L}\rho = -\sum_i \gamma(a_i^\dagger a_i \rho + \rho a_i^\dagger a_i)/2$, where γ is the decay constant determined by the coupling strength of the system and environment, and a_i is the annihilation operator for mode i.

The formal solution of Eq. (6.3) is written as $\rho(\tau) = \exp[(\hat{J}+\hat{L})\tau]\rho(0)$, where $\rho(0)$ is the initial density operator at $\tau = 0$. By solving this equation we obtain the decohered density matrix for the initial state of the hybrid channel $|\psi_{pc}\rangle$ in Eq. (6.1) as

$$\begin{aligned}\rho_{pc}(t;\alpha) = \frac{1}{2}\Big[&\big\{ t^2 \left|H\right\rangle_p \left\langle H\right| + (1-t^2)\left|0\right\rangle_p \left\langle 0\right| \big\} \otimes \left|t\alpha\right\rangle_c \left\langle t\alpha\right| \\ &+ \big\{ t^2 \left|V\right\rangle_p \left\langle V\right| + (1-t^2)\left|0\right\rangle_p \left\langle 0\right| \big\} \otimes \left|-t\alpha\right\rangle_c \left\langle -t\alpha\right| \\ &+ t^2 Q(t) \big(\left|H\right\rangle_p \left\langle V\right| \otimes \left|t\alpha\right\rangle_c \left\langle -t\alpha\right| + h.c. \big) \Big]\end{aligned} \tag{6.4}$$

where the parameter $t = e^{-\gamma\tau/2}$ describes the amplitude decay, and $Q(t) \equiv e^{-2\alpha^2(1-t^2)}$ reflects the reduction of the off-diagonal coherent-state dyadic $|\alpha\rangle\langle -\alpha|$ and its hermitian conjugate. We define the normalized time as $r = (1-t^2)^{1/2}$ which gives a value $r = 0$ at $\tau = 0$ and $r = 1$ at $\tau = \infty$. Likewise, we obtain the

decohered density matrix $\rho_{ps}(t)$ for the initial state in the channel in Eq. (6.2) as

$$\begin{aligned}\rho_{ps}(t) = \frac{1}{2}\Big[&\big\{t^2 \left|H\right\rangle_p \left\langle H\right| + (1-t^2)\left|0\right\rangle_p \left\langle 0\right| \big\} \otimes \left|0\right\rangle_s \left\langle 0\right| \\ &+ \big\{t^2 \left|V\right\rangle_p \left\langle V\right| + (1-t^2)\left|0\right\rangle_p \left\langle 0\right| \big\} \otimes \big\{t^2 \left|1\right\rangle_s \left\langle 1\right| \\ &+ (1-t^2)\left|0\right\rangle_s \left\langle 0\right| \big\} + t^3\big(\left|H\right\rangle_p \left\langle V\right| \otimes \left|0\right\rangle_s \left\langle 1\right| + h.c.\big)\Big]. \end{aligned} \tag{6.5}$$

As shown in Eqs. (6.4) and (6.5), photon loss induces (i) the decay of the amplitude of coherent state as $|\alpha\rangle \rightarrow |t\alpha\rangle$, (ii) the transition of the polarization states $\left|H\right\rangle_p \left\langle H\right|$ and $\left|V\right\rangle_p \left\langle V\right|$ into vacuum state $\left|0\right\rangle_p \left\langle 0\right|$, which causes an escape error out of the qubit space, (iii) the transition of the single photon Fock state $\left|1\right\rangle_s \left\langle 1\right|$ into vacuum state $\left|0\right\rangle_s \left\langle 0\right|$, a flip error of the qubit, and (iv) the decrease of the coefficients of coherence (off-diagonal) terms with $t^2Q(t)$ in Eq. (6.4) and t^3 in Eq. (6.5).

6.3 Entanglement of hybrid channels

The negativity of state ρ, known as a measure of entanglement, is defined as [167, 168]

$$N(\rho) = ||\rho^{T_B}|| - 1 = 2\sum_{\lambda_i<0} |\lambda_i|, \tag{6.6}$$

where ρ^{T_B} is the partial transpose of ρ about one mode of composite system (say mode B here), $||\cdot||$ denotes the trace norm and λ_i's are negative eigenvalues of ρ^{T_B}. We calculate the negativity of the decohered channel ρ_{pc} given in Eq. (6.4)

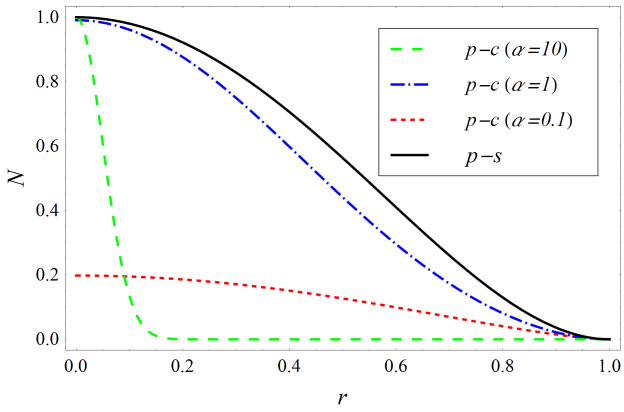

Figure 6.1: Negativity of the hybrid channels, ρ_{pc} (dotted, dot-dashed, and dashed curves) and ρ_{ps} (solid curve) in Eqs. (6.4) and (6.5), against the normalized time r under decoherence.

as

$$N(\rho_{pc}(t;\alpha)) = \frac{(Q(t)-1)(N_+^2+N_-^2)+\sqrt{16Q(t)N_+^2N_-^2+(1-Q(t))^2(N_+^2+N_-^2)^2}}{2t^{-2}N_+^2N_-^2} \tag{6.7}$$

where $N_\pm = (2 \pm 2e^{-2t^2\alpha^2})^{-1/2}$ are normalization factors for equal superpositions of coherent states $|\pm\rangle = N_\pm(|t\alpha\rangle \pm |-t\alpha\rangle)$. This is obtained by representing the coherent state qubit part of Eq. (6.4) in the orthogonal basis $\{|\pm\rangle\}$ and performing calculations following Eq. (6.6). The negativity of the decohered entangled channel ρ_{ps} in Eq. (6.5) is also obtained as

$$N(\rho_{ps}) = t^4. \tag{6.8}$$

The degrees of entanglement for the two channels are plotted in Fig. 6.1, and we find that entanglement contained in $|\psi_{ps}\rangle$ is more robust to decoherence than

that of $|\psi_{pc}\rangle$. Obviously, state $|\psi_{pc}\rangle$ is more entangled when α is larger at the initial time. As $\alpha \to 0$, the initial state approaches a product state with no entanglement. However, when the initial value of α is larger, the slope of the decrease of entanglement is steeper, *i.e.*, entanglement disappears more rapidly. The reason for this is that state $|\psi_{pc}\rangle$ becomes a more "macroscopic" quantum superposition, fragile to decoherence, when α is large. This feature has been pointed out in a number of previous studies [170, 147, 172, 171, 173] with various versions of continuous-variable superpositions and entangled states. In our case, when $\alpha \approx 1$, entanglement seems most robust to decoherence considering both the initial value and the decrease slope of entanglement.

6.4 Teleportation between polarization and coherent-state qubits

We now consider quantum teleportation using the hybrid channels. Besides the hybrid channels, a Bell-state measurements and single-qubit unitary transforms, σ_x and σ_z operations, at the receiver's site are required to complete the teleportation process. In order to avoid unrealistic assumptions, we assume throughout the chapter that only linear optics elements are available besides the hybrid quantum channels.

In this Section, we first investigate quantum teleportation between polarization and coherent state qubits through the decohered entangled state ρ_{pc} in Eq. (6.4). For convenience, we use the arrow $A \to B$ for the teleportation from qubit type A to type B when a hybrid entangled state composed of two qubits

with types A and B is used as the teleportation channel. For example, $p \to c$ indicates teleportation from polarization to coherent-state qubits, and $c \to p$ vice versa.

6.4.1 Teleportation fidelities

The teleportation fidelity F is defined as $F = \langle\psi_{\rm t}|\,\rho_{\rm out}\,|\psi_{\rm t}\rangle$ where $|\psi_{\rm t}\rangle$ is the target state of teleportation and $\rho_{\rm out}$ is the density operator of the output qubit. Due to the nonorthogonality of two coherent states, it is not trivial to define the fidelity between a polarization qubit and a coherent-state qubit. In the case of telportation from a polarization qubit, $|\psi_{\rm t}\rangle_p = a\,|H\rangle_p + b\,|V\rangle_p$, to a coherent state qubit, it would be reasonable to choose the target state as

$$|\psi_{\rm t}\rangle_c = N(a\,|t\alpha\rangle_c + b\,|-t\alpha\rangle_c), \tag{6.9}$$

where $N = \{1 + (ab^* + a^*b)e^{-2t^2\alpha^2}\}^{-1/2}$ is the normalization factor. We note that we take a dynamic qubit basis $\{|\pm t\alpha\rangle\}$ in order to reflect the decrease of the amplitude under photon losses [147], and that t is considered a known value. Conversely, for the teleportation of opposite direction ($c \to p$) the state in Eq. (6.9) is considered the input qubit and $|\psi_{\rm t}\rangle_p = a\,|H\rangle_p + b\,|V\rangle_p$ the target state.

The Bell-state measurement, an essential part of quantum teleportation, dis-

criminates four Bell states:

$$|B_{1,2}\rangle_{pp'} = \frac{1}{\sqrt{2}}(|H\rangle_p |H\rangle_{p'} \pm |V\rangle_p |V\rangle_{p'}), \tag{6.10}$$

$$|B_{3,4}\rangle_{pp'} = \frac{1}{\sqrt{2}}(|H\rangle_p |V\rangle_{p'} \pm |V\rangle_p |H\rangle_{p'}). \tag{6.11}$$

The Bell-state measurement in polarization modes can be performed by a 50:50 beam splitter, two polarizing beam splitters and photon detectors [80], which discriminates only $|B_{3,4}\rangle_{pp'}$ successfully. The net effect of this process is equivalent to taking the inner product of the total density matrix $|\psi_t\rangle_p \langle\psi_t| \otimes \rho_{p'c}(t;\alpha)$ with a Bell state, and an appropriate unitary transform is applied to reconstruct the original state. For example, when one of the Bell states, $|B_1\rangle_{pp'}$, is measured, the output state for the teleportation from a polarization to a coherent state qubit for an input state $|\psi_t\rangle_p$ is given as

$$\rho_{\text{out}}^{p\to c} = \frac{{}_{pp'}\langle B_1| \left\{ |\psi_t\rangle_p \langle\psi_t| \otimes \rho_{p'c}(t;\alpha) \right\} |B_1\rangle_{pp'}}{\text{Tr}\Big[|B_1\rangle_{pp'} \langle B_1| \left\{ |\psi_t\rangle_p \langle\psi_t| \otimes \rho_{p'c}(t;\alpha) \right\} \Big]}. \tag{6.12}$$

In this case, no unitary transform is required. In the cases of the other outcomes, the required unitary transforms for the coherent state part are

$$\begin{aligned} Z_c &: |\pm t\alpha\rangle_c \to \pm |\pm t\alpha\rangle_c , \\ X_c &: |\pm t\alpha\rangle_c \to |\mp t\alpha\rangle_c , \end{aligned} \tag{6.13}$$

after which the state of Eq. (6.12) is obtained. One or both of these operations should be applied depending on the Bell-state measurement outcome [147]. It is relatively easy to perform X_c using phase shifter, while the implementation of

Z_c is non-trivial [147, 152]. The displacement operation can approximate the Z_c operation [147, 149] but it becomes effective only for $\alpha \gg 1$. We shall therefore assume that the outcomes requiring the Z_c operation are discarded, and only $|B_3\rangle_{pp'}$ is taken as a success. Inserting explicit forms of $\rho_{p'c}(t;\alpha)$ in Eq. (6.4) and $|\psi_t\rangle_p = a\,|H\rangle_p + b\,|V\rangle_p$ into (6.12) gives

$$\rho_{\rm out}^{p\to c} = \frac{|a|^2\,|t\alpha\rangle_c\langle t\alpha| + |b|^2\,|-t\alpha\rangle_c\langle -t\alpha| + Q(t)\big(ab^*\,|t\alpha\rangle_c\langle -t\alpha| + a^*b\,|-t\alpha\rangle_c\langle t\alpha|\,\big)}{1+e^{-2\alpha^2}(ab^*+a^*b)}. \tag{6.14}$$

We find the fidelity between the output state $\rho_{\rm out}^{p\to c}$ in Eq. (6.14) and the target state $|\psi_t\rangle_c = N(a\,|t\alpha\rangle_c + b\,|-t\alpha\rangle)_c$ as

$$F_{p\to c} = {}_c\langle\psi_t|\,\rho_{\rm out}^{p\to c}\,|\psi_t\rangle_c = \frac{|a^2+2abS+b^2|^2 + 2(Q(t)-1){\rm Re}\big[(a^2+abS)(abS+b^2)^*\big]}{N^{-2}\Big\{1+e^{-2\alpha^2}(ab^*+a^*b)\Big\}} \tag{6.15}$$

where $S = \langle t\alpha| - t\alpha\rangle = \exp(-2t^2\alpha^2)$ is the overlap between the dynamic qubit basis states.

We now need to find the average teleportation fidelity over all possible input states. In order to obtain the average fidelity, an input state, either $|\psi_t\rangle_p$ or $|\psi_t\rangle_c$ in our study, is parameterized with $a = \cos[\theta/2]\exp[{\rm i}\phi/2]$ and $b = \sin[\theta/2]\exp[-{\rm i}\phi/2]$ where $0 \le \phi < 2\pi$ and $0 \le \theta < \pi$. This parameterization reflects the isomorphism of the states in different physical bases.

We can now obtain the average of $F(\theta,\phi)$ in Eq. (6.15) over all input states

using Eq. (6.17) as

$$F_{p\to c}(t) = \langle F(\theta,\phi)\rangle_{\theta,\phi} = \frac{1}{4\pi}\int_0^{\pi} d\theta \sin\theta \int_0^{2\pi} d\phi F(\theta,\phi)$$
$$= \frac{Q(t)}{Q(t)-1}\Big\{2G[|a|^4] + \big(2S^2 + 2Q(t)\big)G[|a|^2|b|^2]$$
$$+ (SQ(t)+S)G[ab^* + a^*b] + S^2Q(t)G[a^2b^{*2} + a^{*2}b^2]\Big\}, \tag{6.16}$$

where $G[f]$'s for arbitrary value or function f which may contain θ or ϕ are defined as

$$G[f] = \langle \frac{f}{1+Q(t)S(ab^*+a^*b)} - \frac{f}{1+S(ab^*+a^*b)}\rangle_{\theta,\phi}, \tag{6.17}$$

and for arbitrary value x independent of θ and ϕ,

$$\langle \frac{|a|^4}{1+x(ab^*+a^*b)}\rangle_{\theta,\phi} = \frac{x + \frac{-1+3x^3}{\tanh[x]}}{8x^3}, \tag{6.18}$$

$$\langle \frac{|a|^2|b|^2}{1+x(ab^*+a^*b)}\rangle_{\theta,\phi} = -\frac{x + \frac{-1-x^2}{\tanh[x]}}{8x^3}, \tag{6.19}$$

$$\langle \frac{ab^*+a^*b}{1+x(ab^*+a^*b)}\rangle_{\theta,\phi} = \frac{1}{x} - \log[\frac{1+x}{1-x}]\frac{1}{2x^2}, \tag{6.20}$$

$$\langle \frac{a^2b^{*2}+a^{*2}b^2}{1+x(ab^*+a^*b)}\rangle_{\theta,\phi} = \frac{2-x^2}{4x^3}\log[\frac{1+x}{1-x}] - \frac{1}{x^2}. \tag{6.21}$$

Now, we consider teleportation from a coherent state qubit to a polarization qubit. The Bell-state measurement for coherent-state qubits can be performed using a 50:50 beam splitter and two photon number parity measurements [147]. The input qubit of the form of Eq. (6.9) together with the coherent-state part of

channel $\rho_{pc'}(t;\alpha)$ passes through the 50:50 beam splitter and evolves as

$$\begin{aligned}
&\big(a\,|\beta\rangle + b\,|-\beta\rangle\,\big)_c\,|\beta\rangle_{c'} \to a\,|\beta'\rangle_c\,|0\rangle_{c'} + b\,|0\rangle_c\,|\beta'\rangle_{c'} \\
&\big(a\,|\beta\rangle + b\,|-\beta\rangle\,\big)_c\,|-\beta\rangle_{c'} \to a\,|0\rangle_c\,|-\beta'\rangle_{c'} + b\,|-\beta'\rangle_c\,|0\rangle_{c'}\,,
\end{aligned} \tag{6.22}$$

where $\beta = t\alpha$ and $\beta' = \sqrt{2}\beta$. We note that the photons move to either of the two modes so that only one of the two detectors can detect any photon(s). The projection operators O_j for the outcomes j of the two parity measurements can then be written as

$$\hat{O}_1 = \sum_{n=1}^{\infty} |2n\rangle_A\langle 2n| \otimes |0\rangle_B\langle 0|, \tag{6.23}$$

$$\hat{O}_2 = \sum_{n=1}^{\infty} |2n-1\rangle_A\langle 2n-1| \otimes |0\rangle_B\langle 0|, \tag{6.24}$$

$$\hat{O}_3 = \sum_{n=1}^{\infty} |0\rangle_A\langle 0| \otimes |2n\rangle_B\langle 2n|, \tag{6.25}$$

$$\hat{O}_4 = \sum_{n=1}^{\infty} |0\rangle_A\langle 0| \otimes |2n-1\rangle_B\langle 2n-1|, \tag{6.26}$$

where subscripts 1, 2, 3 and 4 represent four Bell states

$$|\mathcal{B}_{1,2}\rangle_{cc'} \propto |\alpha_c\rangle_{c'}|\alpha\rangle \pm |-\alpha\rangle_c|-\alpha\rangle_{c'}, \tag{6.27}$$

$$|\mathcal{B}_{3,4}\rangle_{cc'} \propto |\alpha_c\rangle_{c'}|-\alpha\rangle \pm |-\alpha\rangle_c|\alpha\rangle_{c'}, \tag{6.28}$$

respectively. In addition, the error projection operator $\hat{O}_{\rm e} = |0\rangle_A\langle 0| \otimes |0\rangle_B\langle 0|$ should also be considered because there is possibility for both the detectors not to register anything, even though such probability approaches zero for $\alpha \gg 1$.

In the calculation to obtain the output density matrix when the element of the parity measurement $\hat{O}_1$ is measured, the terms such as $|0\rangle_c |\beta'\rangle_{c'}$ and $|0\rangle_c |-\beta'\rangle_{c'}$ in Eq. (6.22) are erased from the resultant density matrix due to the orthogonality of vacuum state in these terms and non-zero number states contained in $\hat{O}_1$. Other terms form the same factor $\sum_{n=1}^{\infty}\langle 2n|\beta'\rangle\langle\pm\beta'|2n\rangle = \cosh(\beta'^2) - 1$, which is factored out into the normalization factor. When $\hat{O}_2$, $\hat{O}_3$ and $\hat{O}_4$ are measured in the parity measurements, the unitary transforms required are Pauli matrices $(\sigma_z)_p$, $(\sigma_x)_p$ and $(\sigma_y)_p$ in the basis set of $\{|H\rangle, |V\rangle\}$, respectively.

The overall effect of the Bell-state measurement and unitary transform is found to be replacement of $|t\alpha\rangle_{c'}$ ($\langle t\alpha|_{c'}$) with a (a^*) and $|-t\alpha\rangle_{c'}$ ($\langle -t\alpha|_{c'}$) with b (b^*) in the teleportation channel $\rho_{pc'}(t;\alpha)$ in Eq. (6.4). We obtain after the normalization

$$\begin{aligned}\rho_{\rm out}^{c\to p} =& \frac{{\rm Tr}_{cc'}\left[(\hat{O}_1 U_{\rm BS})_{cc'}(\rho_{pc'}(t;\alpha)\otimes|\psi_{\rm t}\rangle_c\langle\psi_{\rm t}|)(U_{\rm BS}^\dagger)_{cc'}\right]}{{\rm Tr}\left[(\hat{O}_1 U_{\rm BS})_{cc'}(\rho_{pc'}(t;\alpha)\otimes|\psi_{\rm t}\rangle_c\langle\psi_{\rm t}|)(U_{\rm BS}^\dagger)_{cc'}\right]} \\ =& t^2|a|^2|H\rangle_p\langle H| + t^2|b|^2|V\rangle_p\langle V| + (1-t^2)|0\rangle_p\langle 0| \\ &+ t^2 Q(t)\big(ab^*|H\rangle_p\langle V| + a^*b|V\rangle_p\langle H|\big), \end{aligned} \tag{6.29}$$

where $U_{\rm BS}$ represents the beam splitter operator. The fidelity is then

$$F_{c\to p}(\theta,\phi) = {}_p\langle\psi_{\rm t}|\,\rho_{\rm out}^{c\to p}\,|\psi_{\rm t}\rangle_p = t^2\big(|a|^4 + |b|^4 + Q(t)|a|^2|b|^2\big) \tag{6.30}$$

and its average can be calculated in a similar way as Eq. (6.16)

$$F_{c\to p}(t) = t^2\left(\frac{2}{3} + \frac{Q(t)}{3}\right). \tag{6.31}$$

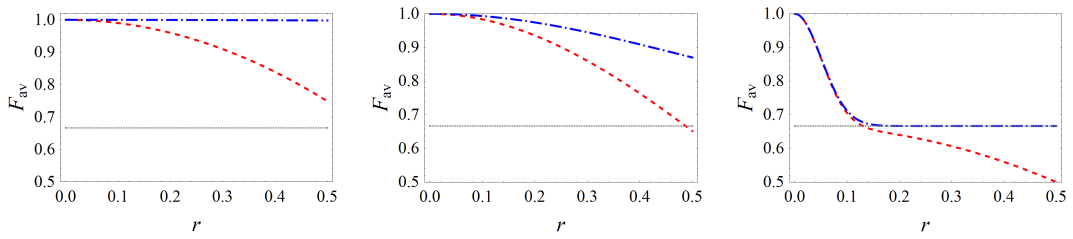

(a) $\alpha = 0.1$ (b) $\alpha = 1$ (c) $\alpha = 10$

Figure 6.2: Average fidelities of teleportation from polarization to coherent state qubits ($p \to c$, dot-dashed curves) and of teleportation in the opposite direction ($c \to p$, dashed curves) for several values of α. The classical limit 2/3 is plotted for comparison (horizontal lines).

In Fig. 6.2, we plot the time evolution of average teleportation fidelities for different coherent state amplitudes $\alpha = 0.1, 1, 2, 10$ against the normalized time r. For large α, the teleportation fidelities of both directions $p \leftrightarrow c$ decrease rapidly down to the classical limit 2/3 after short time evolution due to the fast decay of entanglement in the channel as shown in Fig. 6.1. For small α, the average fidelity is significantly larger than the classical limit in both directions ($p \to c$ and $c \to p$) in spite of the small amount of entanglement contained in the channel as shown in Fig. 6.1. Moreover, if we compare the results of $\alpha = 0.1$ and $\alpha = 1$, we can observe that the teleportation via the channel with smaller entanglement ($\alpha = 0.1$) shows a higher fidelity for teleportation. This result can be understood as the effect of nonorthogonality between coherent states $|t\alpha\rangle$ and $|-t\alpha\rangle$, meaning that a qubit carries information with an nonorthogonal basis. Nevertheless, information encoded in the nonorthogonal basis does not necessarily imply loss of information. In fact, when an input qubit either of polarization or of coherent states is teleported to the other side and teleported back through a

channel of Eq. (6.5) with $\alpha \ll 1$, the outcome state is the same to the original state as far as there is no loss.

In our analysis, as implied in Fig. 6.2, the fidelity of teleportation from polarization to coherent state qubit ($p \to c$) is shown to be always larger than that of teleportation in the opposite direction ($c \to p$). In the region over the classical limit 2/3, the gap between these two fidelities for a given r decreases as α becomes larger as shown in Fig. 6.2. This gap can be obtained and explained as follows. In the limit of large α, the output state of the teleportation ($p \to c$) in Eq. (6.14) can be approximated as

$$\rho_{\text{out}}^{p\to c} \approx |a|^2 \left|t\alpha\right\rangle_c \left\langle t\alpha\right| + |b|^2 \left|-t\alpha\right\rangle_c \left\langle -t\alpha\right| + Q(t)(ab^* \left|t\alpha\right\rangle_c \left\langle -t\alpha\right| + a^* b \left|-t\alpha\right\rangle_c \left\langle t\alpha\right|). \tag{6.32}$$

The comparison between the output state for $p \to c$ in Eq. (6.32) and the output state for $c \to p$ in Eq. (6.29) shows that the difference even for large values of α can be attributed to the term $(1-t^2)\left|0\right\rangle_p \left\langle 0\right|$ in Eq. (6.29). The fidelity between the output state in Eq. (6.32) and the target state $\left|\psi_{\text{t}}\right\rangle_c$ is given as $|a|^4 + |b|^4 + 2Q(t)|a||b|$ and its average can be calculated to be $(2+Q(t))/3$. By subtracting Eq. (6.31) from this, we obtain the gap between the two fidelities as $(1-t^2)(2+Q(t))/3$. In the limit of $\alpha \to \infty$, the gap at time t_{cl} that satisfies $F_{c\to p}(t_{cl}) = 2/3$ approaches zero.

The difference between $F_{p\to c}$ and $F_{c\to p}$ observed in Fig. 6.2 can be explained by two effects: (i) the overlap between $|t\alpha\rangle$ and $|-t\alpha\rangle$ which is dominant at the region $t\alpha \ll 1$, and (ii) the effect that the polarization qubit turns into the vacuum state by photon loss so that the output can no longer be in the original qubit

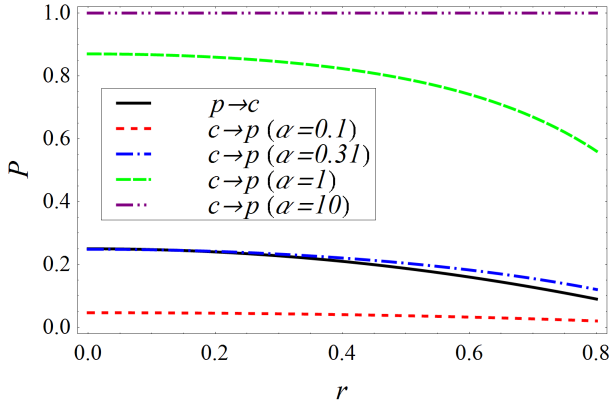

Figure 6.3: Success probability for teleportation between polarization and coherent qubits for different coherent state amplitudes ($\alpha = 0.1, 1, 0.31, 10$) against the normalized evolving time under decoherence r.

space: this is not the case for the dynamic qubit basis using $|\pm t\alpha\rangle$. In the case of $p \to c$, the vacuum introduced by photon loss is detected during the Bell-state measurement and discarded by virtue of its particle nature. This filtering effect in the Bell-state measurement for the polarization qubits enhances the fidelity $F_{p\to c}$ over $F_{c\to p}$. From the fact that the teleportation through dephasing channel always shows a higher fidelity than the classical limit 2/3, it can be explained that the average fidelity of teleportation $p \to c$ is always higher than the classical limit as shown in Fig. 6.2. For $c \to p$, the average fidelity is lowered below the classical limit as the vacuum component comes into the output state.

6.4.2 Success probabilities

An event of the teleportation process should be discarded either when the Bell-state measurement fails or when the appropriate unitary transform is unavailable. Due to these discarded events, the success probability of the teleportation process

becomes smaller than unity. We first consider the teleportation of $p \to c$. The Bell-state measurement for the teleportation of $p \to c$ is to distinguish the four Bell states of polarization qubits. This type of Bell-state measurement can identify only two of the four Bell states, $|B_3\rangle_{pp'}$ and $|B_4\rangle_{pp'}$ [80].

When $|B_4\rangle_{pp'}$ is observed in the Bell measurement, the joint application of Z_c and X_c are required in the receiver's station, while only X_c is necessary for the case of $|B_3\rangle_{pp'}$. As explained in the previous subsection, we take only $|B_3\rangle_{pp'}$ as a success and discard all the other results. Considering these inherent limitations, the success probability of teleportation $p \to c$ cannot exceed 1/4. Beside these, a failure of the Bell-state measurement also occurs when the photon is lost from the channel in the polarization qubit part. Such loss can be immediately noticed at the detectors used for the Bell-state measurement and should be considered for the success probability.

The success probability for a specific input state is

$$P(\theta,\phi) = \mathrm{Tr}\left[\, |B_3\rangle_{pp'} \langle B_3| \left\{ |\psi_{\mathrm{t}}\rangle_p \langle \psi_{\mathrm{t}}| \otimes \rho_{p'c}(t;\alpha) \right\} \right] = t^2(1 + A\sin\theta\cos\phi)/4. \tag{6.33}$$

In fact, the explicit form of $P(\theta,\phi)$ is obtained during the normalization of the output state $\rho_{\mathrm{out}}^{p\to c}$ as the inverse of the normalization factor as implied in Eqs. (6.12) and (6.14). The total success probability over all of the input states can be calculated by

$$P_{p\to c}(t) = \langle P_{p\to c}(\theta,\phi)\rangle_{\theta,\phi} = \frac{t^2}{4}, \tag{6.34}$$

On the other hand, teleportation for $c \to p$ can be performed with a high

probability close to unity only using linear optics. This is due to the two reasons as follows. First, the Bell-state measurement for the coherent-state qubits, required for the sender's site in this process, can discriminate between all four Bell states [147]. Second, the single-qubit unitary transforms for the polarization qubit, to be performed in the receiver's site, are straightforward for any outputs. The results are discarded only when no photons are detected in the Bell-state measurement. Of course, when loss caused by decoherence occurs, the parity measurement scheme used in the Bell-state measurements cannot filter out "wrong results" in the polarization part, which is obviously different from the Bell-state measurement with polarization qubits, and this type of errors will be reflected in the degradation of the fidelity.

The success probability of $c \to p$ teleportation for a given input state is then obtained by

$$P_{c\to p}(\theta,\phi) = \sum_i \langle U_{\rm BS}^\dagger \hat{O}_i U_{\rm BS}\rangle = (1-S)/(1+S\sin\theta\cos\phi) \tag{6.35}$$

where $\hat{O}_i$'s are the projection operators introduced in the previous subsection and $U_{\rm BS}$ is the operator for 50:50 beam splitter. The success probability of all input states can be calculated in the same way described above and the result is

$$P_{c\to p}(t) = \frac{S^{-1}-1}{2}\log\left(\frac{1+S}{1-S}\right). \tag{6.36}$$

The success probabilities in Eqs. (6.34) and (6.36) are plotted and compared for several values of α in Fig. 6.3. The success probability $P_{p\to c}(t)$ is invariant under the change of α, while $P_{c\to p}(t)$ becomes larger as α increases. As the hybrid

channel undergoes decoherence, both $P_{p\to c}(t)$ and $P_{c\to p}(t)$ decrease due to photon losses. The decrease of $P_{c\to p}(t)$ becomes negligible for $\alpha \gg 1$ as the proportion of the vacuum state in the coherent state is very small. When $\alpha \approx 0.31$, probabilities $P_{p\to c}(t)$ and $P_{c\to p}(t)$ become comparable for all ranges of r.

6.5 Teleportation between polarization and single-rail Fock state qubits

In this Section, we go on to investigate teleportation between polarization and single-rail Fock state qubits ($p \leftrightarrow s$) using the hybrid state $\rho_{ps}(t)$ in Eq. (6.5). Let us first consider teleportation from a polarization qubit to a single-rail Fock state qubit ($p \to s$). When $|B_1\rangle_{pp'}$ is detected in the Bell-state measurement for input state $|\psi_t\rangle_p = a\,|H\rangle_p + b\,|V\rangle_p$, the output state obtained similarly as in Eq. (6.12) becomes

$$\rho_{B_{1,2}}^{p\to s} = |a|^2\,|0\rangle_s\langle 0| + |b|^2t^2\,|1\rangle_s\langle 1| + |b|^2(1-t^2)\,|0\rangle_s\langle 0| + t(ab^*\,|0\rangle_s\langle 1| + a^*b\,|1\rangle_s\langle 0|), \tag{6.37}$$

and no unitary transform is required. If $|B_2\rangle_{pp'}$ is measured, the required single qubit operation is $(\sigma_z)_s$ on the corresponding qubit basis to reconstruct state $\rho_{B_{1,2}}^{p\to s}$ in Eq. (6.37). A phase shifter, described by $\exp[i\varphi a^\dagger a]$ with $\varphi = \pi$, can be used to perform this operation. When $|B_3\rangle_{pp'}$ or $|B_4\rangle_{pp'}$ is detected (which is not possible by the Bell measurement of [80] as the success probability cannot exceed 1/2), however, the $(\sigma_x)_s$ operation is also required to implement the bit flip: $|0\rangle \leftrightarrow |1\rangle$, which is not straightforward using linear optics.

We thus take only $|B_1\rangle_{pp'}$ and $|B_2\rangle_{pp'}$ as successful Bell measurement outcomes. The probability to obtain either of these outcomes is found to be

$$P_{p\to s}(\theta,\phi) = \mathrm{Tr}\big[(|B_1\rangle_{pp'}\langle B_1| + |B_2\rangle_{pp'}\langle B_2|)\{|\psi_{\mathrm{t}}\rangle_p\langle\psi_{\mathrm{t}}|\otimes\rho_{p's}(t;\alpha)\}\big] = t^2/2 \tag{6.38}$$

and it is independent of the input state. The fidelity of state of Eq. (6.37) to the target state $|\psi_t\rangle_s = a|0\rangle_s + b|1\rangle_s$ is

$$F_{p\to s}(a,b) =_s \langle\psi_t|\rho_{B_{1,2}}^{p\to s}|\psi_t\rangle_s = |a|^4 + |b|^4t^2 + (1-t^2)|a|^2|b|^2 + 2t|a|^2|b|^2. \tag{6.39}$$

The average fidelity is obtained similarly as Eq. (6.16)

$$F_{p\to s}(t) = \frac{t^2+2t+3}{6}. \tag{6.40}$$

Let us now consider the teleportation in the opposite direction $s \to p$. We consider the Bell measurement in the single-rail Fock state qubit part (implied in [161]) which is performed as follows. With a 50:50 beam splitter, the following transformation may take place: $|B_4\rangle_{ss'} = 2^{-1/2}(|1\rangle_s|0\rangle_{s'} - |0\rangle_s|1\rangle_{s'}) \to |0\rangle|1\rangle$ and $|B_3\rangle_{ss'} = 2^{-1/2}(|1\rangle_s|0\rangle_{s'} + |0\rangle_s|1\rangle_{s'}) \to |0\rangle|1\rangle$, and these two correspond to two Bell states that are easily discriminated from each other by photo-detectors. Other Bell states correspond to indistinguishable results. For Bell measurement outcomes $|B_{3,4}\rangle_{ss'} = (|0\rangle_s|1\rangle_{s'} \pm |1\rangle_s|0\rangle_{s'})/\sqrt{2}$, the output state after the unitary

transformations is

$$\rho_{B_{3,4}} = \frac{t^4|a|^2 + t^2(1-t^2)|b|^2}{4P_3} |H\rangle_p \langle H| + \frac{t^2|b|^2}{4P_3} |V\rangle_p \langle V| + \frac{t^2(1-t^2)|a|^2 + (1-t^2)(2-t^2)|b|^2}{4P_3} |0\rangle_p \langle 0| + \frac{t^3\big(ab^* |H\rangle_p \langle V| + a^* b |V\rangle_p \langle H|\big)}{4P_3}. \tag{6.41}$$

with probability $P_{3,4}(\theta,\phi) = ((2-t^2)|b|^2 + t^2|a|^2)/4$.

The fidelity with the state $|\psi_t\rangle_p = a|H\rangle_p + b|V\rangle_p$ is given as

$$F_{s\to p}(\theta,\phi) = {}_p\langle\psi_t| \rho_{B_{3,4}} |\psi_t\rangle_p = \frac{t^4|a|^4 + t^2(1+2t-t^2)|a|^2|b|^2 + t^2|b|^4}{4P_3}, \tag{6.42}$$

and finally we find the average fidelity over all possible input states similarly as Eq. (6.16),

$$F_{s\to p}(t) = t^4 A_1 + t^2 A_2 + t^2(1+2t-t^2)A_3, \tag{6.43}$$

where

$$\begin{aligned} A_1 &= \langle \frac{|a|^4}{4P_3} \rangle_\theta = \frac{c_1^2 - 4c_1c_2 + 3c_2^2 + 2c_2^2 \log[\frac{c_1}{c_2}]}{2(c_1-c_2)^3}, \\ A_2 &= \langle \frac{|b|^4}{4P_3} \rangle_\theta = \frac{-3c_1^2 + 4c_1c_2 - c_2^2 + 2c_1^2 \log[\frac{c_1}{c_2}]}{2(c_1-c_2)^3}, \\ A_3 &= \langle \frac{|a|^2|b|^2}{4P_3} \rangle_\theta = \frac{c_1^2 - c_2^2 - 2c_1c_2 \log[\frac{c_1}{c_2}]}{2(c_1-c_2)^3} \end{aligned} \tag{6.44}$$

with $c_1 = t^2$ and $c_2 = 2-t^2$. Here θ-average is performed as $\langle\rangle_\theta = 2^{-1}\int_0^\pi \mathrm{d}\theta \sin\theta$, and $a = \cos[\theta/2]\exp[\mathrm{i}\phi/2]$ and $b = \sin[\theta/2]\exp[-\mathrm{i}\phi/2]$. The success probability is $P_{s\to p}(t) = \langle P_{3,4}(\theta,\phi)\rangle_{\theta,\phi} = 1/2$.

We plot the teleportation fidelities in Fig. 6.4(a) and the success probabilities

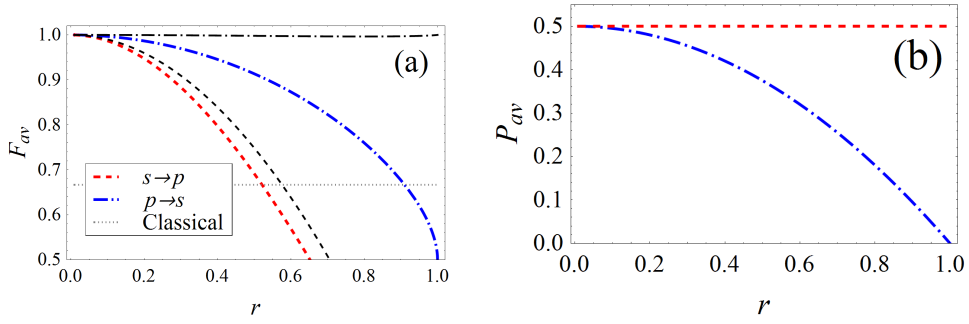

Figure 6.4: (a) Teleportation fidelities of polarization to single-rail Fock state qubit $p \to s$ (blue dot-dashed) and the opposite $s \to p$ (red dashed). Teleportation fidelities of polarization to coherent-state qubit (black dot-dashed) and the opposite direction (black dashed) are drawn for comparison. (b) Success probability of teleportation of polarization to single-rail Fock state qubit $p \to s$ (blue dot-dashed) and the opposite $s \to p$ (red dashed).

in Fig. 6.4(b). We observe that the teleportation fidelity of $p \to s$ is higher than that of $s \to p$ as the loss in polarization qubit (escape effect) can be detected and removed during the Bell measurement, while its success probability is thus lowered as shown in Fig. 6.4 (b). The teleportation $s \to p$ succeeds by 1/2 regardless of r because any decohered single-rail Fock state qubit remains within the qubit space (and the failure occurs only by discarding half of the Bell measurements). We compare the fidelities of $p \leftrightarrow s$ and $p \leftrightarrow c$ for $\alpha = 0.1$ as seen in Fig. 6.4. We observe that the teleportation fidelity of $p \leftrightarrow c$ is always higher than that of $p \leftrightarrow s$ as evolving under decoherence, although $p - s$ channel contains more entanglement for a given time r than $p - c$ channel as shown in Fig. 6.1. This can also be understood as the effect of basis overlap in coherent state qubit.

6.6 Single-qubit rotation of coherent state qubit by hybrid strategy

As was pointed in the previous section and in Chap. 3, two optical implementations of QIP have inherent weaknesses, and hybrid architectures can have advantages in overcoming these weaknesses. For example, the Z-rotations given in [149, 150] adopted infinitesimal displacement operations which work as an effective infinitesimal rotation, and the whole rotation angle is chopped down into smaller ones. However, a large number of applications are required in these strategies, and the fidelity is not unity for small coherent amplitude α. In this section, we give an example of new strategies which may bring advantages in this operation.

The idea is simple. As it is very difficult to implement the single qubit operations in coherent state qubits, we use the hybrid teleportation channel of Eq. (6.1) to transform the coherent state qubit into the polarization qubit and apply the operation here, and then teleport back through the same channel but in different direction to obtain the coherent qubit, but in a form where a single-qubit gate is applied to the original qubit. There can be two strategies to achieve this goal. One is the direct and successive application of teleportation protocols. In this case, we need to apply the Bell measurement in the coherent qubit parts, and then in the polarization parts. However, there exists a danger to destroy the information as the polarization Bell state discrimination in [80] works only probabilistically. Therefore, it is more beneficial to employ the afore-mentioned gate teleportation strategy [17] as depicted in Fig. 6.5.

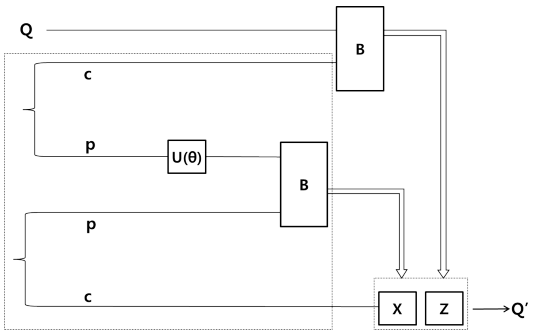

Figure 6.5: It is shown here how the hybrid entangled states can be used to implement the single qubit operation of coherent state qubit. Here the strategy of gate teleportation through hybrid entangled states is depicted. We use two hybrid entangled states in Eq. (6.1), and the initial qubit Q becomes the transformed qubit $Q' = U(\theta)Q$ for single qubit operation $U(\theta)$ after these procedures. The circuit in dotted box is prepared off-line.

The gate teleportation strategy, in short, is an indirect way to implement a gate operation which is difficult to realize experimentally. The key concept is that the operation is applied on the teleportation channel instead of the target qubit, and the actual teleportation is performed on the target qubit we want to apply the operation to only when the operation is successful. A trivial advantage of this strategy is that the probabilistic nature of the operation can be removed as long as the Bell measurement works deterministically. As the Bell measurement in coherent-state QIP works near-deterministically, and the single-qubit operation is difficult to be realized, gate teleportation is a well-suited method for the coherent-state QIP schemes. In fact, the best known method to realize the Z rotation by Lund and co-authors [152] also utilizes the gate teleportation, which prepares the teleportation channel with 1/3 of the success probability, and the fidelity of the operation is unity.

Let us thus take the Z rotation as an example here too. This operation can be written as $Q = a\,|\alpha\rangle + b\,|-\alpha\rangle \rightarrow Q' = U(\theta)Q = a\,|\alpha\rangle + be^{i\theta}\,|-\alpha\rangle$ for coherent state qubits. The teleportation channels used in this gate teleportation strategy is prepared as follows: When Z rotation is applied to the polarization arm of one of the two hybrid entangled channels, the state becomes $2^{-1/2}(|\alpha\rangle\,|H\rangle + e^{i\theta}\,|-\alpha\rangle\,|V\rangle)$. When the polarization Bell measurement is performed for two polarization arms of the transformed channel and another channel, the resultant state becomes

$$\frac{1}{2}(|\alpha\rangle\,|H\rangle + e^{i\theta}\,|-\alpha\rangle\,|V\rangle)(|\alpha\rangle\,|H\rangle + |-\alpha\rangle\,|V\rangle) \rightarrow \begin{cases} B_1: & |\alpha\rangle\,|\alpha\rangle + e^{i\theta}\,|-\alpha\rangle\,|-\alpha\rangle \\ B_2: & |\alpha\rangle\,|\alpha\rangle - e^{i\theta}\,|-\alpha\rangle\,|-\alpha\rangle \\ B_3: & |\alpha\rangle\,|-\alpha\rangle + e^{i\theta}\,|-\alpha\rangle\,|\alpha\rangle \\ B_4: & |\alpha\rangle\,|-\alpha\rangle - e^{i\theta}\,|-\alpha\rangle\,|\alpha\rangle \end{cases} \tag{6.45}$$

As the resultant states corresponding to B_1 and B_3 after the X-flip correction $|\alpha\rangle \leftrightarrow |-\alpha\rangle$ are useful for our goal, while the other resultant states are not, we select only B_1 and B_3 as the successful measurement results. It is possible to discern them by a derivative of the Bell measurement of [80], using two additional Hadamard gates. We can notice that the success probability of the channel preparation is 1/2, enhanced from the value 1/3 of the previous best known result. There exist also a hidden advantage. Our strategy works for arbitrary single-qubit unitary rotations besides Z-rotation with a single-shot teleportation, while it is non-trivial to realize this general unitary rotations using the strategy of Lund *et al.*'s.

There still exist experimental difficulties to realize our proposal. To adopt the strategy used in [152], we have to use the coherent state superposition $|+\rangle =$

$|\beta\rangle + |-\beta\rangle$ where $\beta = \sqrt{2\alpha^2 + 1/2}$, which is extremely difficult to generate when α is large because $\beta > \alpha$. In order to use the coherent amplitude $\alpha = 1.3$, we have to use $|+\rangle$ with $\beta = 1.97$, which exceeds the current reach of experimental realizations. On the other hand, in order to generate the state $|H\rangle |\alpha\rangle + |V\rangle |-\alpha\rangle$ we need to use a huge cross-Kerr nonlinearity if α is large.

6.7 Remarks

We have investigated quantum teleportation between two different types of optical qubits under the effects of decoherence: one type is particle-like such as photon polarization qubit and the other is field-like such as coherent state or Fock state qubits. This is motivated from the fact that each type of optical qubit have their own advantages and disadvantages in implementing quantum information processing so that it may be desirable to transfer information between them in hybrid quantum architecture. We also showed an example of how this hybrid quantum teleportation can be used to realize the advantage in qubit gate operations.

We found that the quality of performance of teleportation indicated by the teleportation fidelity and the success probability depends on the direction of the teleportation. The average fidelity of teleportation from particle-like to field-like qubits is shown to be larger than the opposite direction under decoherence. This is due to the asymmetric effect of photon losses in the hybrid channel, as well as due to the possibility of detecting losses in measurements. If we consider the teleportation $p \to c$ we can detect and discard the loss of photons during the Bell

measurement in the polarization qubit part by virtue of its particle nature, which enhance the teleportation fidelity. In addition, even with a teleportation channel containing very small entanglement, it is possible to obtain a large teleportation fidelity by filtering failures of Bell measurements.

The non-orthogonality of coherent state qubit also affects significantly the teleportation fidelity. For example, the teleportation fidelity of $p \to c$ with small α is always higher than that with larger α due to the larger overlap of qubit basis for small α. Due to this effect, it is also observed that the teleportation fidelity of $p \leftrightarrow c$ is always higher than that of $p \leftrightarrow s$ as evolving under decoherence, irrespectively of the contained entanglement in the channel.

On the other hand, teleportation from field-like to particle-like qubits can be more efficient in terms of the success probability. For example, for the teleportation $c \to p$, the success probability of Bell-state discrimination increases as the amplitude of coherent state qubit gets large. Furthermore, single qubit operations in the polarization qubit part can be straightforwardly performed. Note that, as shown in Fig. 6.3 or Fig. 6.4, the enhanced fidelity by discarding failure events in the teleportation $p \to c$ or $p \to s$ results in its lowered success probability than that of $c \to p$ or $s \to p$.

Besides the cases we reported here, one may consider other types of decoherence model such as dephasing channel. In this model, similarly to the result under dissipation channel the teleportation fidelity of $p \to c$ is always higher than that of $c \to p$, but the gap is only due to the basis overlap of coherent state qubit, while the escape effect and filtering of failure would not appear in this case. For the teleportation $p \leftrightarrow s$ under dephasing, there is no fidelity difference between

$p \to s$ and $s \to p$ because of the absence of the overlap and filtering of failure.

The effect of detection efficiency in the Bell measurement can also be considered. For example, inefficiency of detectors degrades the average fidelity in the teleportation $c \to p$, while the teleportation fidelity of $p \to c$ is unaffected thanks to the filtering of the effects of errors by discarding failures in the Bell measurement just equivalently as for the decoherence effect.

This work may provide useful insight on the general aspect of information transfer between systems of different nature. We showed that the performance of teleportation would significantly depend on the type of input and output qubits so that details of the teleportation procedures should be taken into consideration. This implies that the direction of the teleportation has to be specified in order to say about the quality of hybrid teleportation. Although our study has focused on the teleportation, other schemes for information transfer based on quantum state transfer [174] or remote state preparation [175] are worthwhile to consider. As the thermal qubit or coherent state qubit with large amplitude contain many photons [176, 177], our study would be a possible framework for studying the teleportation between microscopic and macroscopic qubits.

Chapter 7

Conclusion

In this thesis, we have compared two all-optical QIP schemes, and searched for a possibility to utilize the advantages of both of the schemes by means of quantum teleportation under the effect of decoherence. There was a critical value of the coherent amplitude $\alpha \approx 0.8$ under which the teleportation in the coherent state basis is superior to the teleportation in photon polarization basis. When the amplitude is larger than the critical value, the polarization basis teleportation works better for a short decoherence time, but after a while the tendency is reversed, i.e. the coherent state basis teleportation rises over the polarization basis teleportation.

The two teleportation strategies showed a different reaction to the inefficient Bell measurements. The photon polarization teleportation was immune to the inefficiency, while the coherent state teleportation was much affected by it in a similar way to the decoherence effect. This sharp contrast is due to the advantages of photonic encodings, as the gate (in this case the Bell measurement) fails when one of the photons is lost, and the failure is signaled so that the filtering strategy

may work to exclude these cases.

The easiness of the single qubit operations and the difficulty of the two qubit operations of the photonic QIP and the inverse tendency in the difficulties of the coherent state QIP inspired us to use the quantum teleportation as a tool to unite the two optical QIP schemes by sending the quantum information contained in the qubits in both directions. This strategy might work using the hybrid entangled state as the teleportation channel, for which one part is made of the photon polarization qubit and the other part is made of the coherent state qubit. Even though my work dealt only with optical qubits, this strategy to transfer information between different systems via teleportation might be extended to other types of qubits, such as atom-cavity, super-conducting qubits or quantum dots. It was found that when this entangled state suffers decoherence, the two directions of teleportation through this channel begin to show differences. The teleportation of the polarization qubit toward the coherent state qubit side shows better quality than the teleportation of the coherent state qubit due to the filtering of the Bell measurement failures and the overlap effect of the basis states of the coherent state qubit. This result has never been reported in previous works in teleportation as the teleportation is exclusively determined by a quantity called the singlet fraction of the channel [122], and this strange result is a direct consequence of the hybrid nature of the entangled state.

This thesis was aimed at the decoherence effect on the teleportation which is central to the realization of linear optical quantum information processing. This study elucidates the fatal hindrance that might decide the performance of the overall process. The first work, where the performance of the teleportations in-

side the two different optical QIP schemes were compared, gives an insight on the condition when one of the two is superior to the other. Among many QIP existing candidates, it is not clear yet which one is the forefront, thus this work helps to decide which one to choose and when. The second work, the teleportation between the photon polarization qubits and the coherent state qubits, was motivated by the perception of the role as an interface between two different QIP schemes which might be played by the quantum teleportation. This study shows a prospect of the unification of the two schemes to make a more effective scheme and its performance in realistic situations, and the asymmetric information transfer caused by the hybrid natures of the qubits and the decoherence. This work may also be interpreted to have a conceptual implication with respect to the information transfer between microscopic and macroscopic objects.

I believe that these works have contributed to the field of discrete-optical quantum information processing, clarified the degree of difficulty of its experimental realization, and suggested a possible way to improve the current schemes.

Bibliography

[1] W. Thomson, Nature **9**, 441 (1874).

[2] R. Landauer: "Irreversibility and heat generation in the computing process," IBM Journal of Research and Development, vol. 5, pp. 183-191, 1961.

[3] R. Feynman , International Journal of Theoretical Physics **21**, 467 (1982).

[4] C. H. Bennett and G. Brassard, "Quantum Cryptography: Public key distribution and coin tossing", in Proceedings of the IEEE International Conference on Computers, Systems, and Signal Processing, Bangalore, p. 175 (1984)

[5] P. W. Shor, SIAM J. Comput. **26**, 1484 (1997).

[6] L. K. Grover : A fast quantum mechanical algorithm for database search, Proceedings, 28th Annual ACM Symposium on the Theory of Computing, p. 212 (1996).

[7] W. K. Wooters and W. H. Zurek Nature **299**, 802 (1982).

[8] G. C. Ghirardi and T. Weber, IL NUOVO CIMENTO B **78**, 9 (1983).

[9] C. H. Bennett, G. Brassard, C. Crépeau, R. Jozsa, A. Peres,

[10] V. Bužek and M. Hillery, Phys. Rev. A **54**, 1844–1852 (1996).

[11] J. L. O'Brien, Science **318**, 1567 (2007)

[12] P. Kok, W. J. Munro, K. Nemoto, T. C. Ralph, J. P. Dowling, P. Jonathan and G. J. Milburn, Rev. Mod. Phys. **79**, 135 (2007).

[13] R.W. Boyd, J. Mod. Opt. **46**, 367 (1999).

[14] M. Schlosshauer, Rev. Mod. Phys., 76, 1267 (2005).

[15] David P. DiVincenzo, arXiv:quant-ph/0002077 (2000)

[16] P. W. Shor, Phys. Rev. A **52**, R2493 (1995)

[17] D. Gottesman and I. L. Chuang, Nature **402**, 390 (1999).

[18] K. Park and H. Jeong, Phys. Rev. A **82**, 062325 (2010).

[19] R. Horodecki, P. Horodecki, M. Horodecki and K. Horodecki, Rev. Mod. Phys. **81**, 865 (2009).

[20] Letter from Einstein to Max Born, 3 March 1947; The Born-Einstein Letters; Correspondence between Albert Einstein and Max and Hedwig Born from 1916 to 1955, Walker, New York, 1971.

[21] A. Einstein, B. Podolsky, N. Rosen, Phys. Rev. **47**, 777 (1935).

[22] R. F. Werner, Phys. Rev. A **40**, 4277 (1989).

[23] H. Ollivier and W. H. Zurek, Phys. Rev. Lett. **88**, 017901 (2001).

[24] J. F. Clauser, M. A. Horne, A. Shimony and R. A. Holt, Phys. Rev. Lett. **23**, 880 (1969).

[25] A. K. Ekert, Phys. Rev. Lett. **67**, 661 (1991).

[26] M. Żukowski, A. Zeilinger, M. A. Horne and A. K. Ekert, Phys. Rev. Lett. **71**, 4287 (1993).

and W. K. Wootters, Phys. Rev. Lett. **70**, 1895 (1993).

[27] J. S. Bell, Physics **1**, 195 (1964).

[28] J. F. Clauser, M.A. Horne, A. Shimony and R. A. Holt, Phys. Rev. Lett. **23**, 880-884 (1969).

[29] D. Bohm, Phys. Rev. **85**, 166 (1952).

[30] B. S. Cirel'son, Lett. Math. Phys. **4**, 93 (1980).

[31] N. Gisin Phys. Lett. A **154**, 201 (1991).

[32] D. M. Greenberger, M. A. Horne, and A. Zeilinger, in Bell's Theorem, Quantum Theory, and Conceptions of the Universe, edited by M. Kafatos (Kluwer, Dordrecht, 1989).

[33] C. Cinelli, M. Barbieri, R. Perris, P. Mataloni, and F. De Martini, Phys. Rev. Lett. **95**, 240405 (2005).

[34] G. Vallone, E. Pomarico, P. Mataloni, F. De Martini, and V. Berardi, Phys. Rev. Lett. **98**, 180502 (2007).

[35] P. Horodecki and R. Horodecki, Phys. Lett. A **194**, 147 (1994).

[36] R. Horodecki and M. Horodecki, Phys. Rev. A **54**, 1838 (1996).

[37] K. G. H. Vollbrecht, and M. M. Wolf, J. Math. Phys. **43**, 4299 (2002).

[38] M. Horodecki, J. Oppenheim, and A. Winter, Nature **436**, 673 (2005).

[39] A. Peres, Phys. Rev. Lett. **77**, 1413 (1996).

[40] C. H. Bennett, G. Brassard, S. Popescu, B. Schumacher, J. A. Smolin, and W. K. Wootters, Phys. Rev. Lett. **76**, 722 (1996).

[41] M. B. Plenio and S. Virmani, Quantum Inf. Comput. **7**, 1 (2006).

[42] C. H. Bennett, D. P. DiVincenzo, J. A. Smolin, and W. K. Wootters, Phys. Rev. A **54**, 3824 (1996).

[43] G. Vidal, J. Mod. Opt. **47**, 355 (2000).

[44] S. Hill and W. K. Wootters,, Phys. Rev. Lett. **78**, 5022 (1997).

[45] W. K. Wootters, Phys. Rev. Lett. **80**, 2245 (1998).

[46] T. J. Osborne and F. Verstraete, Phys. Rev. Lett. **96**, 220503 (2006).

[47] K. Życzkowski, P. Horodecki, A. Sanpera, and M. Lewenstein, Phys. Rev. A **58**, 883 (1998).

[48] G. Vidal, and R. F. Werner, Phys. Rev. A **65**, 032314 (2002).

[49] H. M. Wiseman, S. J. Jones, and A. C. Doherty, Phys. Rev. Lett. **98**, 140402 (2007).

[50] E. Schrödinger, Naturwiss. **23**, 807 (1935).

[51] Bernhard Wittmann, Sven Ramelow, Fabian Steinlechner, Nathan K. Langford, Nicolas Brunner, Howard Wiseman, Rupert Ursin and Anton Zeilinger, arXiv:1111.0760v3 [quant-ph] (2012)

[52] E. G. Cavalcanti, S. J. Jones, H. M. Wiseman, and M. D. Reid, Phys. Rev. A **80**, 032112 (2009).

[53] W. Heisenberg, Zeitschrift für Physik **43**, 172 (1927).

[54] K. Gottfried, T.-M. Yan, *Quantum mechanics: fundamentals*, Springer-Verlag New York (2003).

[55] B. S. DeWitt, Phys. Today **23**, 30 (1970).

[56] M. Lockwood, Br. J. Philos. Sci. **47**, 159 (1996).

[57] P. Pearle, Phys. Rev. D **13**, 857 (1976).

[58] W. H. Zurek, Rev. Mod. Phys., 75, 715 (2003).

[59] H. D. Zeh, Found. Phys. **1**, 69 (1970).

[60] W. H. Zurek, Phys. Rev. D **24**, 1516 (1981).

[61] A. Elby and J. Bub, Phys. Rev. A **49**, 4213 (1994).

[62] S. M. Barnett and P. M. Radmore, *Methods in theoretical quantum optics*, Oxford University Press Inc., New York (1997).

[63] M. Schlosshauer, *Decoherence and the quantum-to-classical transition*, Springer-Verlag Berlin Heidelberg (2007).

[64] M. Dubé and P. C. E. Stamp, Chem. Phys. **268**, 257 (2001).

[65] S. Nakajima, Prog. Theor. Phys. **20**, 948 (1958).

[66] R. Zwanzig, J. Chem. Phys. **33**, 1338 (1960).

[67] M. Sneep and W. Ubach, JQSRT **92**, 293 (2005).

[68] P. van Loock, N. Lütkenhaus, W. J. Munro, and Kae Nemoto, Phys. Rev. A **78**, 062319 (2008).

[69] H. Rohde, J. Eschner, F. Schmidt-Kaler, and R. Blatt, J. Opt. Soc. Am. B **19**, 1425 (2002).

[70] S. L. Braunstein and P. van Loock, Rev. Mod. Phys. **77**, 513 (2005).

[71] T. P. Spiller, W. J. Munro, S. D. Barrett and P. Kok, Contemporary Physics **46**, 407 (2005)

[72] E. Knill, R. Laflamme and G. J. Milburn, Nature **409**, 46 (2001).

[73] R. Raussendorf, D. E. Browne, and H. J. Briegel , Phys. Rev. A **68**, 022312 (2003).

[74] H. Schmidt and A. Imamoğlu, Opt. Lett. **21**, 1936 (1996).

[75] N. Bogoliubov, J. Phys. (USSR) **11**, 23 (1947)

[76] A. Zeilinger, Am. J. Phys. 49, 882 (1981).

[77] C. K. Hong, Z. Y. Ou, and L. Mandel, Phys. Rev. Lett. **59**, 2044 (1987).

[78] S. Lloyd, Phys. Rev. Lett. **75**, 346 (1995).

[79] L. Vaidman and N. Yoran, Phys. Rev. A **59**, 116 (1999).

[80] N. Lütkenhaus, J. Calsamiglia, and K. A. Suominen, Phys. Rev. A **59**, 3295 (1999).

[81] M. Nielsen and I. Chuang, *Quantum Computation and Quantum Information*, Cambridge: Cambridge University Press (2000).

[82] F. M. Spedalieri, H. Lee, and J. P. Dowling, Phys. Rev. A **73**, 012334 (2006).

[83] P. T. Cochrane, G. J. Milburn and W. J. Munro, Phys. Rev. A **59**, 2631 (1999).

[84] H. Jeong and M. S. Kim, Phys. Rev. A **65**, 042305 (2002).

[85] T. C. Ralph, A. Gilchrist, G. J. Milburn, W. J. Munro and S. Glancy, Phys. Rev. A **68**, 042319 (2003).

[86] E. Schrödinger, Naturwissenschaften **14**, 664 (1926).

[87] H. Jeong, M. S. Kim, and Jinhyoung Lee, Phys. Rev. A **64**, 052308 (2001).

[88] H. Jeong and M. S. Kim, Quantum Information and Computation **2**, 208 (2002).

[89] O. Hirota and M. Sasaki, Quantum Communication, Computing, and Measurement **3**, 359 (2002).

[90] A. Ourjourmtsev, H. Jeong, R. Tualle-Brouri and P. Grangier, Nature **448**, 784 (2007).

[91] C R Myers and T C Ralph, New. Jour. Phys., **13**, 115015 (2011).

[92] K. Nemoto and W. J. Munro, Phys. Rev. Lett. **93**, 250502 (2004).

[93] M. Paternostro, M. S. Kim and P. L. Knight, Phys. Rev. A **71**, 022311 (2005).

[94] A. P. Lund, T. C. Ralph and H. L. Haselgrove, Phys. Rev. Lett. **100**, 030503 (2008)

[95] P. Kok, W. J. Munro, K Nemoto, T. C. Ralph, J. P. Dowling, and G. J. Milburn, Rev. Mod. Phys. **79**, 135 (2007).

[96] T. C. Ralph and G. J. Pryde, Progress in Optics **54**, 209 (2009).

[97] D. Bouwmeester, J.-W. Pan, K. Mattle, M. Eibl, H. Weinfurter and A. Zeilinger, Nature **390**, 575 (1997).

[98] J. Calsimiglia and N. Lütkenhaus, Appl. Phys. B **72**, 67 (2001).

[99] S. J. van Enk and O. Hirota, Phys. Rev. A **64**, 022313 (2001).

[100] D. Wilson, H. Jeong and M. S. Kim, J. Mod. Opt. **49**, 851 (2002); H. Jeong and Nguyen Ba An, Phys. Rev. A **74**, 022104 (2006); H. Jeong, W. Son, M. S. Kim, D. Ahn, and C. Brukner, Phys. Rev. A **67**, 012106 (2003); M. Stobinska, H. Jeong, T. C. Ralph, Phys. Rev. A **75**, 052105 (2007); H. Jeong, Phys. Rev. A **78**, 042101 (2008); C.-W. Lee and H. Jeong, Phys. Rev. A **80**, 052105 (2009); H. Jeong, M. Paternostro, and T. C. Ralph, Phys. Rev. Lett. **102**, 060403 (2009); M. Paternostro and H. Jeong, Phys. Rev. A. **81**, 032115 (2010).

[101] X. Wang, Phys. Rev. A **64**, 022302 (2001).

and S. Glancy, Phys. Rev. A. **68**, 042319 (2003).

[102] Nguyen Ba An, Phys. Rev. A **68**, 022321 (2003). (2008).

[103] Nguyen Ba An, Phys. Lett. A **373**, 1701 (2009).

[104] P. Marek and J. Fiurášek, quant-ph arXiv:1006.3644.

[105] W. P. Schleich, *Quantum Optics in Phase Space*, Wiley-VCH (2001).

[106] C. L. Salter, R. M. Stevenson, I. Farrer, C. A. Nicoll, D. A. Ritchie, and A. J. Shields, Nature **465**, 594 (2010).

[107] A. Ourjoumtsev, H. Jeong, R. Tualle-Brouri and P. Grangier, Nature **448**, 784 (2007).

[108] H. Takahashi, K. Wakui, S. Suzuki, M. Takeoka, K. Hayasaka, A. Furusawa, and M. Sasaki, Phys. Rev. Lett. **101**, 233605 (2008).

[109] T. Gerrits, S. Glancy, T. S. Clement, B. Calkins, A. E. Lita, A. J. Miller, A. L. Migdall, S. W. Nam, R. P. Mirin, and E. Knill, arXiv:1004.2727.

[110] A. P. Lund, H. Jeong, T.C. Ralph, and M.S. Kim, Phys. Rev. A **70**, 020101(R) (2004); P. Marek, H. Jeong, M. S. Kim, Phys. Rev. A **78**, 063811 (2008).

[111] J. S. Neergaard-Nielsen, M. Takeuchi, K. Wakui, H. Takahashi, K. Hayasaka, M. Takeoka, and M. Sasaki, quant-ph arXiv:1002.3211.

[112] E.A. Dauler, A. J. Kerman, B.S. Robinson, J. Mod. Opt. **56**, 364 (2009).

[113] R. Hadfield, Nature Photonics **3**, 696 (2009).

[114] B. C. Sanders, Phys. Rev. A **45**, 6811 (1992).

[115] S. J. D. Phoenix, Phys. Rev. A **41**, 5132 (1990).

[116] M. Horodecki, P. Horodecki, and R. Horodecki, Phys. Lett. A **223**, 1 (1996).

[117] G. Vidal and R. F. Werner, Phys. Rev. A, **65**, 032314 (2002).

[118] S. Lee, D. P. Chi, S. D. Oh, and J. Kim, Phys. Rev. A **68**, 062304 (2003).

[119] J. Lee, M. S. Kim, Y.-J. Park, and S. Lee, J. Mod. Opt. **47**, 2151 (2000).

[120] M. S. Kim and V. Bužek, Phys. Rev. A **46**, 4239 (1992).

[121] A direct comparison between arbitrary polarization qubits, $\mu|H\rangle + \nu|V\rangle$, and coherent-state qubits, $\mu|\alpha\rangle + \nu|-\alpha\rangle$, is not straightforward when α is small due to the nonzero overlap between the two component coherent states. It should be noted that we use the orthogonal basis, $|+\rangle$ and $|-\rangle$, for coherent-state qubits in order to calculate the average fidelity for a "fair comparison" with the polarization-qubit case. In this sense, the input coherent-state qubit in comparison to the polarization qubit, $\mu|H\rangle + \nu|V\rangle$, should be considered to be $\mu|+\rangle + \nu|-\rangle$, rather than $\mu|\alpha\rangle + \nu|-\alpha\rangle$, when the overlap $|\langle\alpha|-\alpha\rangle|^2$ is non-negligible.

[122] M. Horodecki, P. Horodecki, and R. Horodecki, Phys. Rev. A **60** 1888 (1999).

[123] K. Hammerer, A. S. Sørensen and E. S. Polzik, Rev. Mod. Phys. **82**, 1041 (2010).

[124] M. A. Nielsen and I. L. Chuang, Quantum Computation and Quantum Information (Cambridge Univ. Press, 2000).

[125] P. Kok, W. J. Munro, K. Nemoto, T. C. Ralph, J. P. Dowling, and G. J. Milburn, Rev. Mod. Phys. **79**, 135 (2007).

[126] J. L. O'Brien, Science **318**, 1567 (2007).

[127] T. C. Ralph and G. J. Pryde, Progress in Optics **54**, 209 (2010).

[128] L. Vaidman and N. Yoran, Phys. Rev. A **59**, 116 (1999).

[129] A. P. Lund, T. C. Ralph, Phys. Rev. A **66**, 032307 (2002). (2002).

[130] P. van Loock, T. D. Ladd, K. Sanaka, F. Yamaguchi, K. Nemoto, W. J. Munro and Y. Yamamoto, Phys. Rev. Lett. **96**, 240501 (2006).

[131] Y. L. Lim, A. Beige and L. C. Kwek, Phys. Rev. Lett. **95**, 030505 (2005).

[132] L. Jiang, C. L. Kane and John Preskill, Phys. Rev. Lett. **106**, 130504 (2011).

[133] H. Jeong, Phys. Rev. A **72**, 034305 (2005).

[134] H. Jeong, Phys. Rev. A **73**, 052320 (2006).

[135] S.-W. Lee and H. Jeong, arXiv:1112.0825v1 (2011).

[136] T. C. Ralph, A. P. Lund and H. M. Wiseman, J. Opt. B: Quantum Semiclass. Opt. **7**, S245 (2005). P. Horodecki, and R. Horodecki, Phys. Lett. A **223**, 1 (1996); J. Lee, M. S. Kim, Y.-J. Park, and S. Lee, J. Mod. Opt. **47**, 2151 (2000).

[137] S. Oh, S. Lee, and H. Lee, Phys. Rev. A **66**, 022316 (2002).

[138] S. Bose, Phys. Rev. Lett. **91**, 207901 (2003).

[139] H.–K. Lo, Phys. Rev. A **62**, 012313 (2000).

[140] H. Jeong and T. C. Ralph, Phys. Rev. Lett. **97**, 100401 (2006).

[141] P. Kok, W. J. Munro, K. Nemoto, T. C. Ralph, J. P. Dowling, and G. J. Milburn, Rev. Mod. Phys. **79**, 135 (2007).

[142] J. L. O'Brien, Science **318**, 1567 (2007).

[143] T. C. Ralph and G. J. Pryde, Progress in Optics **54**, 209 (2010).

[144] E. Knill, R. Laflamme and G. J. Milburn, Nature **409**, 46 (2001).

[145] A. P. Lund, T. C. Ralph, Phys. Rev. A **66**, 032307 (2002).

[146] S. J. van Enk and O. Hirota, Phys. Rev. A **64**, 022313 (2001).

[147] H. Jeong, M. S. Kim, and J. Lee, Phys. Rev. A **64**, 052308 (2001).

[148] H. Jeong and M. S. Kim, Quantum Inf. Comput. 2, 208 (2002).

[149] H. Jeong and M. S. Kim, Phys. Rev. A **65**, 042305 (2002).

[150] T. C. Ralph, A. Gilchrist, G. J. Milburn, W. J. Munro, and S. Glancy, Phys. Rev. A **68**, 042319 (2003).

[151] H. Jeong and T.C. Ralph, arXiv:quant-ph/0509137 Schrodinger Cat States for Quantum Information Processing, in *Quantum Information with Continuous Variables of Atoms and Light* (Imperial College Press) (2006).

[152] A. P. Lund, T. C. Ralph, and H. L. Haselgrove, Phys. Rev. Lett. **100**, 030503 (2008).

[153] K. Nemoto and W. J. Munro, Phys. Rev. Lett. **93**, 250502 (2004).

[154] W. J. Munro, Kae Nemoto, and T. P. Spiller, New J. Phys. **7**, 137 (2005).

[155] H. Jeong, Phys. Rev. A **72**, 034305 (2005).

[156] H. Jeong, Phys. Rev. A **73**, 052320 (2006).

[157] P. van Loock, W. J. Munro, Kae Nemoto, T. P. Spiller, T. D. Ladd, Samuel L. Braunstein, and G. J. Milburn, Phys. Rev. A 78, 022303 (2008).

[158] P. van Loock, Laser & Photonics Reviews **5**,167 (2011).

[159] S.-W. Lee and H. Jeong, arXiv:1112.0825v1 (2011).

[160] C. H. Bennett, G. Brassard, C. Crépeau, R. Jozsa, A. Peres and W. K. Wootters, Phys. Rev. Lett. **70**, 1895 (1993).

[161] T. C. Ralph, A. P. Lund and H. M. Wiseman, J. Opt. B: Quantum Semiclass. Opt. **7**, S245 (2005).

[162] C. C. Gerry, Phys. Rev. A 59, 4095 (1999).

[163] J. H. Shapiro, Phys. Rev. A **73**, 062305 (2006).

[164] J. H. Shapiro and M. Razavi, New J. Phys. **9**, 16 (2007).

[165] J. Gea-Banacloche, Phys. Rev. A **82**, 043823 (2010).

[166] S. J. D. Phoenix, Phys. Rev. A **41**, 5132 (1990).

[167] K. Życzkowski, P. Horodecki, A. Sanpera and M. Lewenstein, Phys. Rev. A **58**, 883 (1998); A. Peres, Phys. Rev. Lett. **77**, 1413 (1996); M. Horodecki, P. Horodecki, and R. Horodecki, Phys. Lett. A **223**, 1 (1996); J. Lee, M. S. Kim, Y.-J. Park, and S. Lee, J. Mod. Opt. **47**, 2151 (2000).

[168] G. Vidal and R. F. Werner, Phys. Rev. A **65**, 032314 (2002).

[169] K. Park and H. Jeong, Phys. Rev. A **82**, 062325 (2010).

[170] M. S. Kim and V. Bužek, Phys. Rev. A 46, 4239 (1992).

[171] H. Jeong, J. Lee, and M. S. Kim, Phys. Rev. A 61, 052101 (2000).

[172] D. Wilson, H. Jeong, and M. S. Kim, J. Mod. Opt., **49**, Special issue for QEP 15, 851 (2002).

[173] J. Park, M. Saunders, Y.-I. Shin, K. An, and H. Jeong, Phys. Rev. A **85**, 022120 (2012).

[174] S. Bose, Phys. Rev. Lett. **91**, 207901 (2003).

[175] H.-K. Lo, Phys. Rev. A **62**, 012313 (2000).

[176] H. Jeong and T. C. Ralph, Phys. Rev. Lett. **97**, 100401 (2006).

[177] H. Jeong and T. C. Ralph, Phys. Rev. A **76**, 042103 (2007).

국문초록

오랫동안 정보란 것은 유용하지만 물리적 실체를 가지지 않는, 물리 법칙과 무관한 어떤 것이라고 생각되어왔다. 그러나 비트의 삭제에 수반하는 엔트로피에 관한 란다우어의 법칙은 이 믿음이 사실이 아니라고 암시한다. 최근의 양자정보처리의 발전은 절재적으로 안전한 통신, 소인수 분해와 데이터베이스 검색의 지수적인 가속과 같은 고전적인 방법으로 접근할 수 없는 장점을 가져왔다.

빛을 정보 전달자로 사용하는 광학적 양자정보처리는 광자 조작의 상당한 진전에 힘입어 다양한 후보 중 인기있는 선택이 되어 왔다. 이와 더불어, 빛을 사용할 때 통신과 연산을 결합하는 것이 용이하다. 상태의 에너지를 보존하는 수동적 광학 요소(예: 빛 나누개)만을 이용하는 선형 광학은 자연적으로 발생하는 비 선형성이 매우 작기 때문에 흥미를 끌고 있다.

다루고 있는 계의 개방성에 의해 일어나는 결 깨어짐은 최근 양자 물리에서 고전성의 발생의 주된 요소로서 여겨지고 있다. 결깨어짐은 정보의 양자적 측면에서 필수 불가결한 결맞음성을 깨뜨리며, 때문에 양자정보처리의 큰 장애물이다.

본 학위 논문에서는 광학적 양자정보 처리에 일어나는 결깨어짐 효과, 특히 베넷 등에 의해 제안된 양자 텔레포테이션에 초점을 맞춘다. 양자 텔레포테이션은 양자 게이트 연산자를 구현하는 매우 효율적인 방법이며, 따라서 그것에

일어나는 퇴화는 전 양자 회로의 효율에 영향을 미칠 것이다.

나는 이 주제와 관련하여 두가지 연구를 소개하려고 한다. 첫째로, 우리는 실용적인 양자정보처리를 위해 얽힌 결맞음 상태와 얽힌 광자 쌍의 비교를 연구한다. 우리는 양자 정보처리에 매우 유용한 것으로 알려진 얽힌 결맞음 상태와 얽힌 광자쌍에 대해 결깨어짐 효과와 측정 효율을 비교한다. 광자 손실에 의한 결깨어짐 효과가 강할 때, 텔레포테이션 양자 채널로서의 얽힌 결맞음 상태는 얽힌 광자쌍을 충실도와 성공 확률의 기준에서 능가한다. 반면, 비효율적 측정기가 사용될 때 얽힌 결맞음 상태는 충실도의 감소를 가져오는 측정되지 않은 실수를 겪는 반면, 얽힌 광자쌍을 사용한 텔레포테이션 설계는 그렇지 않다. 우리의 연구는 현실적인 조건하에서 실제적인 양자정보처리의 구현에 있어 두 종류의 얽힘 상태의 장점과 단점을 드러낸다.

둘째로, 우리는 "입자와 같은" 큐비트와 "마당과 같은" 큐비트의 두 종류의 광학적 큐비트 사이의 양자 텔레포테이션을 연구한다. 우리는 입자와 같은 큐비트에서 마당과 같은 큐비트로의 텔레포테이션이 그 반대 방향에서 보다 더 큰 충실도로 달성될 수 있다는 것을 발견할 수 있다. 그러나 성공 확률의 관점에서는 마당과 같은 큐비트에서 입자와 같은 큐비트가 더 효율적인 것으로 밝혀졌다. 우리의 연구는 양자 정보처리를 위한 광학적 하이브리드 얼개를 개발하는 데 있어 텔레포테이션의 방향이 중요한 요소로 고려되어야 한다는 것을 보여준다.

Keywords: 양자정보처리, 양자 텔레포테이션, 결깨어짐, 광학적 양자 통신

Student Number: 2006-30768

감사의 글

짧지 않은 시간을 대학과 대학원에서 보내면서 제가 가장 많이 느낀 것은, 마치 작은 언덕을 다 오르면 더욱 높은 산이 나타나듯이, 하나의 과정을 힘겹게 마치고 나면 더욱 길고 힘든 과정이 나타나는 것이었습니다. 또한 자만했던 나의 능력이 우스워보일 만큼 대단한 능력을 갖춘 사람들을 보며 느낀 부러움도 그 중 하나였습니다. 처음 시작할 때에는 상상조차 하지 못한, 이루고 나면 끝이라고 생각이 들 것만 같던 박사 학위를 받게 되는 지금, 제가 크게 느끼는 것은 이제 겨우 시작이구나 하는 점입니다. 이것들을 느끼는 것 만으로도 저에겐 큰 성취라고 생각합니다.

긴 시간 동안 부족한 저를 도와주신 많은 분들께 감사드립니다. 그리고 아직도 더 긴 날 들을 기다려주실 분들께 송구스런 마음이 앞섭니다. 이렇게 감사의 말을 드리는 것으로 제게 베풀어주신 도움에 대해 제가 느끼는 감사의 마음을 다 표현할 수 있는지 모르겠습니다.

가장 먼저 저의 박사과정을 지도해 주시고 또한 양자정보 및 양자광학의 길로 인도해 주신 정현석 교수님께 감사의 말씀 드립니다. 교수님의 가르침이 없었다면 저의 부족함을 많이 채우지 못했을 것이라고 생각합니다. 처음부터 지금까지도 교수님의 날카로운 논리와 판단력은 저에게 많은 귀감을 주고 있습니다. 교수님이 아니었다면 학문의 길을 계속할 수 없었을 것이라 생각합니다.

논문을 쓸 때 그리고 연구를 할 때 항상 올바른 길을 추구할 수 있도록 노력하겠습니다.

고등학교 시절부터 저의 롤 모델이셨고 저의 석사 과정을 지도해 주시고 깊은 통찰력과 지식으로 저에게 깊은 감동을 주신 임지순 교수님께 감사드립니다. 부족한 저를 계속 연구의 길을 갈수 있도록 지도해 주시고 존경의 마음을 갖게 해주셔서 다시 한 번 감사드립니다.

저의 중학교 시절 과학반을 지도해 주셨던 유병일 선생님, 저희에게 올바름을 가르쳐 주시려 엄하신 모습 뒤에 저희를 아껴주셨던 마음을 아직 기억 속에 남아있습니다. 선생님의 건강이 쾌차하시길 늘 기도하고 있습니다. 대학원 과정 중에 저의 진로 결정에 큰 도움을 주신 이준규 교수님께 감사드립니다. 교수님께서 보여주신 학자로서의 모습은 저에게 큰 가르침이 되었습니다. 안경원 교수님께서 보여주신 수업에서의 명쾌한 설명은 저에게 매우 인상적이었습니다. 감사합니다. 심사 과정에서 좋은 질문과 지적을 해주신 신용일 교수님, 김형도 교수님께 깊은 감사드립니다. 한양대학교에 계신 이진형 교수님께도 심사를 맡아주셔서 감사드립니다. 교수님과의 토론에서 느끼는 교수님의 진지함과 독특한 생각들은 제가 닮고 싶은 모습입니다. 또한 따뜻한 격려도 늘 저에게 힘을 줍니다.

영국에 계시는 주재우 박사님과 저희 연구실의 이승우 박사님께 공동 연구를 같이 할 수 있는 기회를 주신 점 특히 감사드립니다. 두분과의 토론은 늘 많은 생각을 하게 됩니다. 많은 이야기를 나누진 못했지만 항상 열의를 다한 설명을 해주신 방정호 박사님께도 감사드립니다.

저희 연구실의 많은 멤버들, 졸업하신 이창우 박사님, 그리고 일주일에 가장 많은 시간을 함께 보내는 진우,영롱, 민수, 그리고 후배들 승호, 승리, 채연, 이제 박사과정을 시작해야 하는 호용과 혁준에게도 감사의 말씀과 격려 드립니다.

행정실에서 많은 일을 해주신 보람씨에게도 감사드립니다. 응집물리 그룹의 문현, 충현, 영국 형, 근수 형에게도 감사드리며 또한 운동을 같이 한 시간들 감사드립니다. 지혜, 정주, 선정, 미국에 있는 지연, 그리고 이훈경 박사님과 한명준 박사님, 김승철 박사님, 김건 박사님께도 감사드립니다. 중학교 때 많은 시간을 보냈지만 지금은 떨어져 있는, 그리고 각자의 길을 걸어가고 있는 과학반 친구들에게도 우정에 항상 감사드립니다. 한분 한분 이름을 밝히지 않은 수많은 분들께 감사의 말씀 드립니다.

그리고 지금은 멀리 떨어져있지만 많은 시간을 함께했고, 늘 그리워하고 또 고맙게 생각하는 대학친구들, 일영, 순호, 우석, 윤넝, 수연, 재훈, 재욱, 주영, 승엽, 문주, 영주, 지언, 그리고 영범형과 회철형께도 감사의 말씀 드립니다. 친형제와 다름없는 기완형과 그 가족들, 친동생같은 예림 예진 수현, 작은 아버지들과 어머님들, 고모님들, 사촌들, 또 많은 도움을 주신 외삼촌들과 외숙모들께도 깊은 감사 드립니다.

지금 편찮으시지만 현명하시고 굳센 저희 외할머니께도 깊은 감사의 말씀 드리며, 항상 그 고마움과 사랑을 느끼고 있습니다. 빨리 회복하셔서 건강하신 모습을 찾으시기를 간절히 기도 드립니다.

저에게 큰 의지가 되는 지금 힘든 길을 가고 있는 우리 형, 또 정말로 오랜 시간 동안 기다려주셨고, 그리고 앞으로도 늘 함께할, 그 은혜를 다 갚을 길 없는 사랑하는 부모님께도 이 기회를 빌어 감사의 말씀 드립니다. 오랫동안 자식들을 위해 모든 것을 희생하신 마음 늘 잊지 않겠습니다.

마지막으로 지금은 계시지 않은 할머니, 외할아버지께 감사의 마음과 이 논문을 드립니다.